AD-A162 453 SURFACE PLASMON DISPERSION RELATION AND LOCAL FIELD ENHANCEMENT DISTRIBUT (U) STATE UNIV OF NEW YORK AT BUFFALO DEPT OF CHEMISTRY D AGASSI ET AL DEC 85 1/1

UNCLASSIFIED UBUFFALO/DC/85/TR-1 N00014-86-K-0043 F/G 20/6 NL

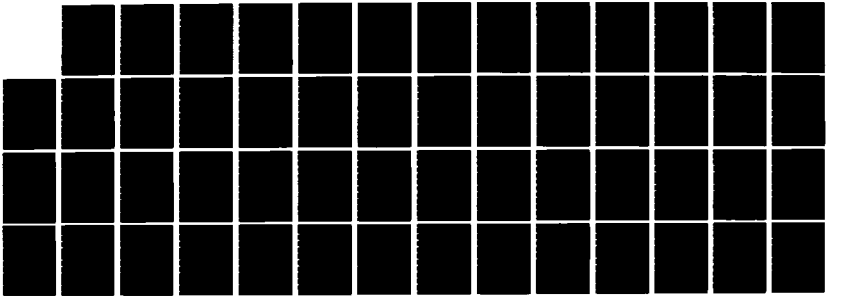

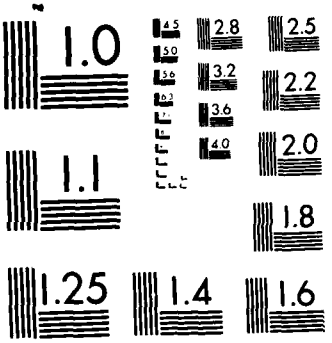

OFFICE OF NAVAL RESEARCH

Contract N00014-86-K-0043

TECHNICAL REPORT No. 1

Surface Plasmon Dispersion Relation and Local Field Enhancement Distribution For a Deep Sinusoidal Grating

by

Dan Agassi and Thomas F. George

Prepared for Publication

in

Surface Science

Departments of Chemistry and Physics
State University of New York at Buffalo
Buffalo, New York 14260

December 1985

UNCLASSIFIED

SECURITY CLASSIFICATION OF THIS PAGE

REPORT DOCUMENTATION PAGE

1a. REPORT SECURITY CLASSIFICATION: Unclassified	1b. RESTRICTIVE MARKINGS
2a. SECURITY CLASSIFICATION AUTHORITY	3. DISTRIBUTION/AVAILABILITY OF REPORT: Approved for public release; distribution unlimited
2b. DECLASSIFICATION/DOWNGRADING SCHEDULE	
4. PERFORMING ORGANIZATION REPORT NUMBER(S): UBUFFALO/DC/85/TR-1	5. MONITORING ORGANIZATION REPORT NUMBER(S)
6a. NAME OF PERFORMING ORGANIZATION: Depts. Chemistry & Physics, State University of New York; 6b. OFFICE SYMBOL (If applicable)	7a. NAME OF MONITORING ORGANIZATION
6c. ADDRESS (City, State and ZIP Code): Fronczak Hall, Amherst Campus, Buffalo, New York 14260	7b. ADDRESS (City, State and ZIP Code): Chemistry Program, 800 N. Qiuncy Street, Arlington, Virginia 22217
8a. NAME OF FUNDING/SPONSORING ORGANIZATION: Office of Naval Research; 8b. OFFICE SYMBOL (If applicable)	9. PROCUREMENT INSTRUMENT IDENTIFICATION NUMBER: Contract N00014-86-K-0043
8c. ADDRESS (City, State and ZIP Code): Chemistry Program, 800 N. Quincy Street, Arlington, Virginia 22217	10. SOURCE OF FUNDING NOS. — PROGRAM ELEMENT NO. / PROJECT NO. / TASK NO. / WORK UNIT NO.

11. TITLE: Surface Plasmon Dispersion Relation and Local Field Enhancement Distribution For a Deep Sinusoidal Grating

12. PERSONAL AUTHOR(S): Dan Agassi and Thomas F. George

13a. TYPE OF REPORT	13b. TIME COVERED	14. DATE OF REPORT (Yr., Mo., Day)	15. PAGE COUNT
Interim Technical	FROM _____ TO _____	December 1985	46

16. SUPPLEMENTARY NOTATION: Physics Letters A

17 COSATI CODES			18. SUBJECT TERMS (Continue on reverse if necessary and identify by block number)
FIELD	GROUP	SUB. GR.	SURFACE PLASMON; DEEP METALLIC GRATING; DISPERSION RELATION; SINUSOIDAL GRATING; LOCAL FIELD ENHANCEMENT; DRESSED RAYLEIGH EXPANSION

19. ABSTRACT (Continue on reverse if necessary and identify by block number)

Two features of light scattering from a deep lossless metallic sinusoidal grating are considered in the limit $g/d \to \infty$, where g and d are the height and periodicity of the grating, respectively. It is found that the surface plasmon dispersion relation is comprised of two flat bands with a frequency gap $\Delta\omega/\omega_p = (\sqrt{2} - 1)/2$, where ω_p is the volume plasmon frequency. For the local field enhancement distribution at the grating's surface, the results show the existence of two qualitatively distinct domains, i.e., $\lambda >> d$ and $\lambda << d$, where λ denotes the radiation wavelength. In both domains, however, the local field enhancement is larger at the bottom of the troughs than at the top of the peaks. The dressed Rayleigh expansion is used throughout for the analysis.

20. DISTRIBUTION/AVAILABILITY OF ABSTRACT	21. ABSTRACT SECURITY CLASSIFICATION	
UNCLASSIFIED/UNLIMITED ☒ SAME AS RPT. ☒ DTIC USERS ☐	Unclassified	
22a. NAME OF RESPONSIBLE INDIVIDUAL: Dr. David L. Nelson	22b. TELEPHONE NUMBER (Include Area Code): (202) 696-4410	22c. OFFICE SYMBOL

DD FORM 1473, 83 APR — EDITION OF 1 JAN 73 IS OBSOLETE.

UNCLASSIFIED

SECURITY CLASSIFICATION OF THIS PAGE

SURFACE SCIENCE, in press

SURFACE PLASMON DISPERSION RELATION AND LOCAL FIELD ENHANCEMENT DISTRIBUTION FOR A DEEP SINUSOIDAL GRATING

Dan Agassi
Naval Surface Weapons Center
White Oak
Silver Springs, Maryland 20910, USA

Thomas F. George
Departments of Chemistry and Physics
State University of New York at Buffalo
Buffalo, New York 14260, USA

Abstract

Two features of light scattering from a deep lossless metallic sinusoidal grating are considered in the limit $g/d \to \infty$, where g and d are the height and periodicity of the grating, respectively. It is found that the surface plasmon dispersion relation is comprised of two flat bands with a frequency gap $\Delta\omega/\omega_p = (\sqrt{2} - 1)/2$, where ω_p is the volume plasmon frequency. For the local field enhancement distribution at the grating's surface, the reults show the existence of two qualitatively distinct domains, i.e., $\lambda >> d$ and $\lambda << d$, where λ denotes the radiation wavelength. In both domains, however, the local field enhancement is larger at the bottom of the troughs than at the top of the peaks. The dressed Rayleigh expansion is used throughout for the analysis.

1. Introduction

Light scattering from a deep grating, i.e., a grating for which $\beta = 2\pi g/d >> 1$ where g and d are the maximum (and minimum) extension and periodicity of the grating, respectively (see Fig. 1), is a relatively newly studied physical phenomenon. Moderately deep gratings can now be fabricated, e.g., by photodissociation of organometallic molecules at a substrate.[1,2] The extremely deep grating case ($\beta \to \infty$), which is at the focus of this work, should be considered as an idealized limit. This limit is complementary to the shallow grating limit ($\beta << 1$), which is realized in many physical systems and has been extensively explored over the last century.

The extremely deep grating regime is qualitatively different from the shallow grating regime.[3] It can be characterized as a strong coupling situation in the sense that the many possible Bragg reflections (Fig. 1) interfere strongly with each other, giving rise to a scattered field of new qualitative features. By contrast, the shallow grating regime can be analyzed in terms of a few 'weak' (in comparison with the specular reflected light) Bragg reflections. Unfortunately, attempts to solve the Maxwell equations for deep gratings using the so-called Rayleigh expansion, which works beautifully when $\beta << 1$, have encountered numerical instabilities.[4] These difficulties have motivated the introduction of several alternative schemes,[1,5,6] all of which, however, share difficulties in the $\beta >>> 1$ regime. In another paper[3] we have suggested yet another scheme -- dubbed as the dressed Rayleigh expansion -- which overcomes these difficulties. We have also explicitly demonstrated[3] that this

scheme converges for a sinusoidal grating (SG) of arbitrary β. Here we apply the dressed Rayleigh expansion to study two aspects of light scattering from a very deep metallic SG grating, namely, the surface plasmon (SP) dispersion relation and the distribution of the local field enhancement along the grating's surface.

Our results are valid in the $\beta \to \infty$ limit and under several approximations which are spelled out as we go along. For the SP dispersion relation we find two flat bands (see Fig. 2). The frequency band gap $\Delta\omega$ is given by $\Delta\omega/\omega_p = \frac{\sqrt{2}-1}{2} = .207$, where ω_p is the volume-plasma frequency of the metal. We interpret the two bands to reflect two classes of localized surface modes -- those for which the field maxima are in the peaks and in the troughs of the grating respectively. A similar situation occurs in standard band structure studies. The fact that we obtain dispersion <u>bands</u> rather than the usual dispersion <u>curves</u> for $\beta \ll 1$ is in keeping with studies of moderately deep gratings, $g/d \lesssim 1$,[7,8] where it has been observed for the latter that as g/d increases new SP dispersion branches pop out in pairs at the $\omega/\omega_p = 1/\sqrt{2}$ line. As g/d keeps increasing, one branch of the pair is pushed upward and the other branch is pushed downward to be followed by the emergence of a new pair of branches. Since the available frequency interval is confined both from below ($\omega/\omega_p = 0$) and from above ($\omega/\omega_p = 1$), the accumulation of the branches into bands as $\beta \to \infty$ may be expected. However, the particular band gap and widths we derive [Eqs. (4.4) and (4.5)] may be, in part, an artifact of our approximations. SP dispersion bands have also been derived for an infinitely large stack of thin metallic films.[9]

We also evaluate a simple figure-of-merit representing the local field enhancement distribution. The local field enhancement R is defined as $R = |\vec{E}/\vec{E}_{inc}|^2$, where $\vec{E}$ is the total electric field and $\vec{E}_{inc}$ is the incident electric field.[6,10] The value and distribution of R are of prime importance in determining optical and chemical processes near the grating.[11] To remain within reach of a simple analytical result, we evaluate only $R(T/B) = |R(T)/R(B)|^2$, where the points T (top) and B (bottom) are defined in Fig. 1, and the incident light is normal to the grating. The result [Eq. (5.3)] indicates the existence of two distinct regimes, i.e., $\lambda >> d$ and $\lambda << d$, where λ is the wavelength of the incident light. The R(T/B) ratio in the former is smaller than in the latter, and in both regimes $R(T/B) \sim 1/\beta$. These findings are understood in terms of the following physical picture: The incident field induces the electrons in the metal into an oscillating motion, and the electrons respond. Since the grating is deep, the motion of the electrons at the grating's peak is inhibited by the grating's boundaries, and much less so at the troughs' bottoms, and hence $R(T/B) << 1$. The distinction between the $\lambda >> d$ and $\lambda << d$ regimes can also be understood in the same vein: The response of the electrons at the bottoms is inhibited by the grating's boundaries and hence depends only mildly on λ. The response of the electrons at the peak's top, however, is strongly dependent on λ: For $\lambda >> d$, these electrons respond very poorly due to the confinement of the grating's boundaries, while, as λ ever decreases, the top electrons can respond ever more efficiently. Consequently, the ratio R(T/B) is larger for $\lambda << d$ than for $\lambda >> d$.

The paper is organized as follows: We introduce in Section 2 the dressed Rayleigh expansion[3] in the context of the SG. In Section 3 we present the central approximations which enable a simple solution for the light scattering problem in the asymptotic limit $\beta \to \infty$. The results of Section 3 are then applied in Section 4 to analyze the SP dispersion relations and in Section 5 to evaluate the local field enhancement distribution for a particularly simple configuration. Section 6 is a discussion and summary.

2. Dressed Rayleigh Expansion and Sinusoidal Grating

We introduce in this section the dressed Rayleigh expansion[3] and the pertinent formulas of the SG. As has been demonstrated elsewhere, the dressed Rayleigh expansion converges for an SG arbitrary β and therefore provides a convenient framework to analyze the $\beta \to \infty$ limit. All expressions in this section are exact. The notations throughout are defined in Fig. 1

The dressed Rayleigh expansion for the electromagnetic fields is[3]

$$\vec{E}_0(x,z) = \sum_{\ell=-\infty}^{\infty} \{\gamma_0(\ell)\hat{p}_{0,-}(\ell)\, e^{i[k_\ell x - W_0(\ell)(z+g)]} + \alpha_0(\ell)\,\hat{p}_{0,+}(\ell)\, e^{i[k_\ell x + W_1(\ell)(z+g)]}\}$$

$$\vec{E}_1(x,z) = \sum_{\ell=-\infty}^{\infty} \gamma_2(\ell)\,\hat{p}_{1,-}(\ell)\, e^{i[k_\ell x - W_1(\ell)(z-g)]} \qquad (2.1.a)$$

and

$$\vec{B}_0(x,z) = \frac{k(0)}{k}\,\hat{s}\sum_{\ell=-\infty}^{\infty}\{\gamma_0(\ell)\,e^{i[k_\ell x - W_0(\ell)(g+z)]} + \alpha_0(\ell)\,e^{i[k_\ell x + W_0(\ell)(g+z)]}\}$$

$$\vec{B}_1(x,z) = \frac{k(1)}{k}\,\hat{s}\sum_{\ell=-\infty}^{\infty}\gamma_1(\ell)\,e^{i[k_\ell x - iW_1(\ell)(g-z)]}, \qquad (2.1.b)$$

where

$$\gamma_0(\ell) = \delta_{\ell,0}\,\bar{E}_{0,p}\,e^{+iW_0(\ell)g} \qquad (2.2)$$

and

$$k(i) = \sqrt{\varepsilon_i}\,k, \qquad k = \omega_0/c, \qquad k_G = 2\pi/d$$

$$W_i(\ell) = [k^2(i) - k_\ell^2]^{1/2}, \qquad k_\ell = k_{||} + \ell k_G$$

$$\hat{p}_{i,\pm}(\ell) = \frac{1}{k(i)}[k_\ell\hat{z} \mp W_i(\ell)\hat{x}], \qquad \hat{s} = \hat{x}\times\hat{z}$$

$$\text{for } i = 0,1\,. \qquad (2.3)$$

In (2.1) - (2.3) the subscripts of the fields refer to the domains (0 or 1), the time dependence of the fields is assumed to be $e^{-i\omega_0 t}$, $k_{||}$ is the $\vec{x}$-momentum component label of the field, $\hat{x}$, $\hat{z}$ and $\hat{s}$ are unit operators in the obvious three directions, $\bar{E}_{0p}$ is the arbitrary amplitude of the p-polarized incident light normal to the grating's grooves, and we always choose $\mathrm{Im}[W_i(\ell)]$ or $\mathrm{Re}[W_i(\ell)] \geq 0$. The height g (positive) is half the maximum z-extension of the grating (Fig. 1), and the central parameter β is again

$$\beta = gk_G\,. \qquad (2.4)$$

The dressed Rayleigh expansion coefficients satisfy

$$\sum_{\ell=-\infty}^{\infty} M_{m,\ell}\,\alpha_0(\ell) = \mu(m)$$

$$\sum_{\ell=-\infty}^{\infty} N_{m,\ell}\,\gamma_1(\ell) = \nu(m)\,, \qquad (2.5.a)$$

where the matrix $\underline{M}$, for instance, can be dubbed as the "Fresnel matrix". It is given by

$$M_{m,\ell} = e^{i(W_1(m) + W_0(\ell)g} M^B_{m,\ell} \quad , \quad \mu(m) = e^{iW_1(m)g} \mu^B(m)$$

$$N_{m,\ell} = e^{i(W_0(m) + W_1(\ell))g} N^B_{m,\ell} \quad , \quad \nu(m) = e^{iW_0(m)g} \nu^B(m) \quad , \tag{2.5.b}$$

and

$$M^B_{m,\ell} = \frac{W_0(\ell)W_1(m) + k_\ell k_m}{W_0(\ell) - W_1(m)} \, i^{m-\ell} \, J_{m-\ell}[g(W_0(\ell) - W_1(m))]$$

$$N^B_{m,\ell} = \frac{W_1(\ell)W_0(m) + k_\ell k_m}{W_1(\ell) - W_0(m)} \, i^{m-\ell} \, J_{m-\ell}[g(-W_1(\ell) + W_0(m))]$$

$$\mu^B(m) = \frac{-W_0(0)W_1(m) + k_0 k_m}{W_0(0) + W_1(m)} \, i^m \, J_m[-g(W_0(0) + W_1(m))] E^-_{0p}$$

$$\nu^B(m) = \frac{2\varepsilon_0\varepsilon_1}{\varepsilon_1 - \varepsilon_0} W_0(m)\delta_{m,0} \, E^-_{0p} \quad , \tag{2.6}$$

where J_ν denotes the Bessel function of order ν.

It has been shown elsewhere[3] that the set of equations (2.5) can be safely truncated at a maximum $|\ell|$-value L of the order β, since the matrix elements of $\underline{M}$ decay exponentially with ℓ or m and become insignificant beyond that point. A more detailed examination reveals that the important matrix elements of $\underline{M}$ are distributed in two lobes: one lobe is for m 'small' and $|\ell|$ 'large' and the other for ℓ 'small' and $|m|$ 'large'. The diagonal terms diminish exponentially with $\ell = m$ faster than either lobe's length.

Once the set of equations (2.5) is solved, all properties of the scattered fields are known. The difficulty when $\beta \to \infty$, however, is that the relevant matrix $\underline{M}$ (or $\underline{N}$) is very large and highly non-diagonal. We

introduce in the next section an asymptotic approximate solution of (2.5) and then explore its implications with regard to the SP dispersion relation and light scattering.

3. Approximate Solution for $\beta >>> 1$

To discuss the fields scattered by the grating, it is necessary to invert the Fresnel matrix $\underline{M}$ [Eq. (2.5)], which has an effective dimensionality on the order of β when $\beta >> 1$. Obviously to gain insight we need to introduce further simplifying approximations. The construction of a simple approximation to $\underline{M}^{-1}$ is the content of this section. The sequence of approximations below that lead to the final result [Eqs. (3.8)-(3.10)] assumes that $\beta >>> 1$, i.e., very deep gratings. At some points we resort to additional approximations motivated by the gained mathematical simplicity. We believe that the plausibility of the results derived in Sections 4 and 5 based on the approximate $\underline{M}^{-1}$ vindicate the approximations. To gain perspective on the $\beta >> 1$ regime considered here, we give the analysis pertaining to shallow gratings in Appendix A.

An attractive feature of $\underline{M}$, or $\underline{M}^{B}$, is its partial separability in the "m" and "ℓ" indices [Eq. (2.6)]. As will become obvious shortly, separable matrices are convenient mathematically. We are therefore motivated to devise a separable approximation to the other factors in (2.6), in particular to the Bessel function factor. This turns out to be possible provided $|m|$, $|\ell|$ and $|m-\ell|$ are very large compared to unity, which is the case for most of the elements of the highly non-diagonal matrix $\underline{M}$.

Using (2.6) the ensuing quasi-separable approximation is (Appendix B)

$$M^{(S)}_{m,\ell} = C_0 \frac{1}{[W_0(\ell) - W_1(m)]^{3/2}} i^{m-\ell}[W_0(\ell)W_1(m) + k_\ell k_m]$$

$$\times e^{ig[W_0(\ell) + W_1(m)]} \{e^{i\Phi} + e^{-i\Phi}\} , \qquad (3.1.a)$$

where

$$C_0 = \sqrt{\frac{\overline{k_G}}{2\pi}} \frac{1}{(1 + \beta^2)^{1/4}}$$

$$\Phi = \frac{\eta(\beta)}{k_G}[W_0(\ell) - W_1(m)] - [\frac{m - \ell}{2} + \frac{1}{4}]\pi$$

$$\eta(\beta) = \sqrt{1 + \beta^2} + \ln[\beta/(1 + \sqrt{1 + \beta^2})] \quad . \qquad (3.1.b)$$

The above is valid for $|m|, |\ell|, |m-\ell| >> 1$. It can be easily checked by comparison with (2.6) that (3.1) provides a surprisingly good approximation even for the diagonal element $M_{\ell,\ell}$.

Note that $M^{(S)}$ has a separable form except for the denominator $[W_0(\ell)-W_1(m)]^{3/2}$. This is to be expected since a fully separable form for $M^{(S)}$ does not possess an inverse. To maintain the simplicity of a separable approximation on the one hand and yet to secure the existence of a simple inverse on the other hand, we introduce the following additional approximation: Consider first the off-diagonal matrix elements of $M^{(S)}$. These elements are grouped into two lobes (Section 2), i.e., when $|m|$ is 'small' and $|\ell|$ is 'large', and vice versa. When $|m|$ is 'small' and $|\ell|$ is 'large', for example, the fastest $|\ell|$-changing factor in $M^{(S)}$ is the exponential [Eq. (3.1)]. Consequently, the above mentioned now separable denominator, which changes with $|\ell|$ much more

slowly, acts approximately as a normalizing factor. It can be therefore approximated by a suitably chosen constant, denoted by C_1. For the sake of simplicity, we further approximate $[W_0(\ell)-W_1(m)]^{3/2} \approx C_1$ for both the $|m| << |\ell|$ and $|\ell| << |m|$ elements. The diagonal elements of $M^{(S)}$ comprise the complementary (minority) group of elements to the off-diagonal elements just discussed. In this case, the above argument concerning the fastest $|\ell|-|m|$-changing factor in $M^{(S)}$ is still valid. However, the corresponding constant approximating the non-separable denominator is obviously quite different, i.e., $[W_0(\ell)-W_1(\ell)]^{3/2} \approx C_2$. The foregoing discussion suggests therefore the approximation

$$M_{m,\ell} \simeq M^{(S)}_{m,\ell} = D_\ell \, \delta_{m,\ell} + V_{m,\ell} \quad , \tag{3.2}$$

$$V_{m,\ell} = C \, i^{m-\ell}[W_0(\ell)W_1(m) + k_\ell k_m] e^{ig[W_0(\ell) + W_1(m)]} \{e^{i\Phi} + e^{-i\Phi}\}$$

$$C = C_0/C_1 \quad , \tag{3.3}$$

and C_1 has been defined in the discussion above.

The diagonal elements D_ℓ in Eq. (3.2) depend, of course, on the choice of C_1 and C_2. However, regardless of the particular choice, due to the convergence factors $e^{ig[W_0(\ell) + W_1(m)]}$, the number of significant diagonal elements is of the order of unity. Therefore, there are only very few significant diagonal terms in comparison with the number of off-diagonal terms, yet if they are neglected, Eq. (3.2) ceases to have an inverse. We have therefore a situation where a few diagonal terms are not important in terms of physical results, yet due to the particular mathematical structure (separability) it is necessary to keep them to assure the existence of an inverse. Under such

conditions, it is probably immaterial as to how the diagonal terms are chosen, provided the calculated observable does not depend on the specifics of the choice. We therefore simplify Eq. (3.2) further by the approximation $D_\ell = D$, where D is a very small number of the order $e^{-\beta}$ or less. Again, to be consistent with the arguments above, we can use the ensuing approximation only to calculate observables that do not depend on D, such as those analyzed in the next two sections. We would like to emphasize that the $D_\ell = D$ approximation is not essential, i.e., it is possible to invert Eq. (3.2) as it stands. The substantial simplification gained by adopting this approximation, however, warrants an examination. Therefore, Eq. (3.2) is replaced by

$$M_{m,\ell} = D\delta_{m,\ell} + V_{m,\ell} \tag{3.4}$$

where D is a very small number of the order $e^{-\beta}$.

The inversion of Eq. (3.4) can be obtained now in a straightforward manner. Note from Eq. (3.3) that V is comprised of four separable terms,

$$V_{m,\ell} = \sum_{j=1}^{4} a_j(m)\, b_j(\ell) \ , \tag{3.5}$$

where the factors a_j and b_j are extracted from Eqs. (3.1.b) and (3.3) [see Appendix C, Eq. (C.2)]. The form of Eq. (3.5) has the attractive property that V to the n-th power is given by

$$(V^n)_{m,\ell} = \sum_{i,j=1}^{4} a_j(m)[A^{n-1}]_{i,j}\, b_j(\ell) \ , \tag{3.6}$$

where the auxiliary interaction matrix $\underline{A}$ is of dimension 4 with the elements

$$A_{i,j} = \sum_{\ell=-\infty}^{\infty} b_i(\ell) a_j(\ell) \ . \tag{3.7}$$

The auxiliary matrix $\underline{A}$ (Appendix C) plays a central role in all subsequent manipulations. Consequently, expanding the inverse of Eq. (3.4) in a geometric series and using Eq. (3.6) yields

$$(M^{-1})_{m,\ell} = \frac{1}{D}\,\delta_{m,\ell} - \frac{1}{D^2}\sum_{i,j=1}^{4} a_i(m)\left([1 + \frac{1}{D}A]^{-1}\right)_{i,j}\, b_j(\ell)$$

$$= \frac{1}{D}\left[\delta_{m,\ell} - \sum_{i,j=1}^{4} a_i(m)[A^{-1}]_{i,j}\, b_j(\ell)\right] \quad . \qquad (3.8)$$

The second line in Eq. (3.8) follows since $\langle|\underline{A}|\rangle/D$, where $\langle|\underline{A}|\rangle$ is a typical average value of the elements of $\underline{A}$ [see (C.18) and (C.20)] and D is an extremely small number.

The approximate inverse (3.8) is a key result of this work. The unknown parameter D appears as a multiplicative factor, implying that (3.8) can be used only to evaluate ratios so that D drops out from the final result. Note that (3.8) embodies the reduction of an inversion problem of a $\beta \times \beta$ matrix to the inversion of a 4×4 matrix.

Based on the analytical expressions for the matrix elements of $\underline{A}$ (Appendix C), the inverse $\underline{A}^{-1}$ can be further simplified. The key remark is that when $\beta \to \infty$, the matrix elements denoted by "α" in Table 1 are substantially smaller than the rest of $\underline{A}$ [see (C.11) and following discussion] and therefore can be neglected. Consequently,

$$\det(\underline{A}) = \det(\underline{A}_\gamma)\,\det(\underline{A}_\delta)$$

$$\det(\underline{A}_\gamma) = A_{1,2}\,A_{3,4} - A_{1,4}\,A_{3,2}$$

$$\det(\underline{A}_\delta) = A_{2,1}\,A_{4,3} - A_{2,3}\,A_{4,1} \quad , \qquad (3.9)$$

where the symbol "det" indicates a determinant, and

$$\underline{A}^{-1} = \frac{1}{\det(\underline{A}_\gamma)} \begin{pmatrix} 0 & 0 & 0 & 0 \\ A_{3,4} & 0 & -A_{1,4} & 0 \\ 0 & 0 & 0 & 0 \\ -A_{3,2} & 0 & A_{1,2} & 0 \end{pmatrix}$$

$$+ \frac{1}{\det(\underline{A}_\delta)} \begin{pmatrix} 0 & A_{4,3} & 0 & -A_{2,3} \\ 0 & 0 & 0 & 0 \\ 0 & -A_{4,1} & 0 & A_{2,1} \\ 0 & 0 & 0 & 0 \end{pmatrix} \quad (3.10)$$

+ mixed γ and δ terms

The simplicity of (3.9) and (3.10) in conjunction with (3.8) is most gratifying. It indicates an expectation that in the limit $\beta \ggg 1$, as in the $\beta \ll 1$ limit, the physics should simplify. All that is needed to obtain $\underline{M}^{-1}$ are eight matrix elements, combined in the simple form of (3.10)!

4. Surface Plasmon Dispersion Relation

Surface plasmon excitations are collective, surface-attached oscillations of the metal's electron gas, well studied in the context of flat metallic surfaces and shallow gratings.[7,8] For the case of a shallow grating, the dispersion relation is comprised of many branches (for a lossless metal, as assumed here throughout) which are arranged in pairs above and below the line $k/k_p = \sqrt{2}$, where $k_p = \omega_p/c$ and ω_p is the volume plasmon frequency. In this section we derive the dispersion relation for the $\beta \to \infty$ limit, i.e., pertaining to very deep gratings.

The emergence of pairs of dispersion relation branches when $\beta \neq 0$ can be understood using arguments employed in interpreting the opening of a band gap for electrons moving in a periodic ionic potential.[12] In

the latter case there are two interfering combinations of unperturbed electron wave and the umklapp-reflected wave. Since one combination is centered at the ions' sites and the other between ions, the associated energy of these two combinations are split and a band gap opens. In the present case the Bragg reflections play the role of the umklapp processes and the unperturbed electron waves -- by the flat-surface SP mode (see Appendix A)and hence the pairs of dispersion branches. We expect this type of dichotomy to persist for $\beta \to \infty$. The remaining issue is therefore how do these pairs of branches accumulate for $\beta \to \infty$, given that the available frequency domain is bounded from below by $\omega/\omega_p = 0$ and from above by $\omega/\omega_p = 1$.

By definition, the SP excitations decay exponentially in both z-directions, Fig. 1, i.e., these are excitations for which $E^{-}_{0p} = 0$ in (2.6). Consequently, to have a non-trivial solution of the Fresnel equations (2.5), the condition

$$\det(\underline{M}) = 0 \tag{4.1}$$

determines a function of k(0) versus $k_{||}$ provided that $-k_G/2 \leq k_{||} \leq k_G/2$, i.e., $k_{||}$ is confined to the first Brillouin zone.[7] Condition (4.1) is tantamount to finding the points where $\underline{M}^{-1}$ does not exist (poles). Hence, in the context of the approximate inverse (3.8), Eq. (4.1) transcribes into $\det(\underline{A}) = 0$. The determinant of $\underline{A}$, however, is given by (3.9) in the leading asymptotic order. Consequently, since $\det(\underline{A}_\delta) \neq 0$ outside the light cone [see Eq. (C.22)], the SP dispersion relation is simply

$$\det(\underline{A}_\gamma) = A_{1,2}\, A_{3,1} - A_{1,4}\, A_{3,2} = 0 \tag{4.2}$$

Inserting into (4.2) the explicit expressions for the matrix elements (C.20) yields

$$\frac{[3k^2(0) + k^2(1))(k^2(0) + 3k^2(1)]}{3[k^2(0) + k^2(1)]^2}$$

$$= \left[\frac{\sin[L(\alpha + \gamma)]\sin[\frac{\alpha - \gamma}{2}] - \sin L[(\alpha - \gamma)]\sin[\frac{\alpha + \gamma}{2}]}{\sin[L(\alpha + \gamma)]\sin[\frac{\alpha - \gamma}{2}] + \sin[L(\alpha - \gamma)]\sin[\frac{\alpha + \gamma}{2}]}\right]^2 , \qquad (4.3.a)$$

where $k(i) = \sqrt{\varepsilon_i}\, k$ from (2.2) and

$$\gamma = 2\pi k / k_G$$

$$\alpha = \frac{\pi}{k_G}\{-[k^2(0) + k^2(1)]\}^{1/2} . \qquad (4.3.b)$$

In (4.3.a) L is a very large number of the order β [see the discussion after Eq. (C.12)], the precise value of which is immaterial (see below).

The analysis of (4.3) is quite simple. Consider first the $k(0) \leq k_p/[1 + \varepsilon_0]^{1/2}$ regime, where α and obviously γ of (4.3.b) are real and hence the RHS of (4.3.a) is real and positive. It can be easily shown that for (4.3.a) to have a solution it is necessary that $k < k_p/[3\varepsilon_0 + 1]^{1/2}$. When $k(0) \geq k_p/[1 + G_0]^{1/2}$ the α-parameter is imaginary and hence the RHS of (4.3.a) is real and negative. Simple considerations show again that

to make the LHS of (4.3.a) negative it is necessary that $k < [\frac{3}{3 + \varepsilon_0}]^{1/2} k_p$

in order for a solution to (4.3) to exist, it is necessary that (assuming $\varepsilon_0 = 1$ for simplicity)

$$0 \leq k \leq \frac{k_p}{2} , \qquad \frac{k_p}{\sqrt{2}} \leq k \leq \frac{\sqrt{3}}{2} k_p . \qquad (4.4)$$

Condition (4.4), however, is also sufficient. Since $L \sim \beta >>> 1$, the RHS exhibits oscillations which are ever increasing in amplitude and

frequency as β is increased. Therefore, any k-value within the admissible ranges (4.4) generates a solution of (4.3), i.e., the dispersion relation constitutes two bands (Fig. 2). The frequency gap $\Delta\omega$ between the bands is according to (4.4)

$$\frac{\Delta\omega}{\omega_p} = \frac{\sqrt{2} - 1}{2} . \tag{4.5}$$

The results (4.4) and (4.5) describe the accumulation of dispersion branch pairs mentioned in the beginning of this section. The interpretation of the two bands is identical to that of the two members of a dispersion branch pair: The two bands are comprised, respectively, of modes in which the field is mostly localized either in the troughs or in the peaks of the grating. We cannot be sure at this point to what degree the particular band gap (4.5) and band widths are an artifact of our approximations. At the very least, (4.4) and (4.5) indicate domains of high density of dispersion-relation curves.

Note that the dispersion relation (4.3) or (4.4) does not depend on g, k_G or $k_{||}$. The independence of g or k_G can be understood as follows: If $\beta \to \infty$ is interpreted as $g \to \infty$ and d finite, then obviously the result of any observable cannot depend on g in the asymptotic region. By the same token, the limit $\beta \to \infty$ can be construed as keeping g finite but letting $d \to 0$, which leads again to the conclusion that the result cannot depend, to the leading order, on k_G. The independence of the band structure of $k_{||}$ may be an artifact of our approximations. The behavior of the matrix elements of $\underline{M}$ near the light cone, for instance, is controlled by the $W_j(\ell)$ sectors [Eq. (2.2)], with the square-root feature playing an essential role (Appendix A). On the other hand, in all manipulations employed here, we expand the square root $W_1(\ell)$ as

$$W_1(\ell) = i\left[|k_\ell| - \frac{k^2(j)}{2}\frac{1}{|k_\ell|}\right] , \qquad (4.6)$$

which destroys the regardation effects near the light cone.

5. Local Field Enhancement Distribution for Normal Incident Light

As a second application of our central approximation (3.8), we turn now to the calculation of the local field enhancement distribution at the grating's surface. The local field enhancement R(x,z) is defined as $R(x,z) = \left|\frac{\vec{E}_{0(x,z)}}{E_{0p}^-}\right|^2$. It measures the collective response of the electrons in the metal to an incident electromagnetic field, and is of obvious importance in determining optical and scattering processes near the grating.[11] To simplify the analysis, we pick the simplest configuration. We assume normal incidence of the p-polarized light and consider the ratio of the local field enhancements at the top of the peak to that at the bottom of the trough (points T and B in the notation of Fig. 1). This ratio, denoted by R(T/B), is a convenient figure-of-merit describing the local field enhancement distribution. Since R(T/B) is a ratio of two fields, the unknown constant D in (3.8) does not enter the final expressions.

Combining (3.8), (3.10), (2.5) and (2.1), it is straightforward to obtain for the electric field in region 0 (Fig. 1)

$$\vec{E}_0(x,z) = \gamma_0(0)e^{i[k_0x - W_0(0)z]}\hat{p}_{0,-}(0)$$

$$+ \frac{1}{D}\Big[\Big\{\sum_{\ell=-\infty}^{\infty}\hat{p}_{0,+}(\ell)\, e^{i[k_\ell x + W_0(\ell)z]}\mu(\ell)$$

$$- \sum_{j,n=1}^{4}\Big\{\sum_{\ell=-\infty}^{\infty}\hat{p}_{0,+}(\ell)\, e^{i[k_\ell x + W_0(\ell)z]}a_j(\ell)\Big\}(\underline{A}^{-1})_{j,n}\Big\{\sum_{m=-\infty}^{\infty}b_j(m)\mu(m)\Big\}\Big]$$

$$= \vec{E}_{inc}(x,z) + \vec{E}_f(x,z) + \vec{E}_s(x,z) \quad . \tag{5.1}$$

The decomposition of $\vec{E}_0(x,z)$ in the last line of (5.1) reflects the structure of (3.10): The first term in (3.10), involving the matrix elements $A_{1,2}$, $A_{1,4}$, etc. (or class-γ elements in the terminology of Appendix C and Table 1) gives rise to field components that vary very rapidly with small changes in either k, $k_{\parallel}$ or k_G, etc. This feature is manifested in the explicit expressions for these matrix elements [Eq. (C.20)] and has been exploited already in conjunction with the SP dispersion relation (Section 4). The corresponding component in the total field is denoted by $\vec{E}_f(x,z)$, where the subscript "f" indicates "fast". The second term in (3.10) involving the elements $A_{2,1}$, $A_{2,3}$, etc. (class-δ in the terminology of Appendix C and Table 1) changes slowly with small changes in k, $k_{\parallel}$, etc. and gives rise to the "slow" component in the total field, denoted by $\vec{E}_s(x,z)$ in (5.1). The incident field, denoted by $\vec{E}_{inc}(x,z)$, is the first term on the LHS of (5.1). The decomposition (5.1) of the total field into a fast oscillating component $\vec{E}_f(x,z)$ and a slow envelope $\vec{E}_s(x,z)$ is expected due to the many interfering components (Bragg reflections) of which $\vec{E}_0(x,z)$ is comprised.

In terms of the decomposition (5.1), we identify the ratio of the local field enhancements at points T and B in Fig. 1 with the field envelope, or average:

$$R(T/B) = \left|\frac{\vec{E}_{inc}(T) + \vec{E}_s(T)}{\vec{E}_{inc}(B) + \vec{E}_s(B)}\right|^2 \approx \left|\frac{\vec{E}_s(T)}{\vec{E}_s(B)}\right|^2 , \tag{5.2}$$

where the arguments "T" and "B" in (5.2) indicate the coordinates of points T and B. Straightforward yet somewhat lengthy algebra (Appendix D) gives

$$R(T/B) \approx \frac{r}{4\beta} \quad \text{for } r \ll 1$$

$$\approx \frac{r^7}{4\beta} \quad \text{for } r \gg 1 \tag{5.3}$$

and ($\varepsilon_0 = 1$ for simplicity)

$$r = \frac{k(0)}{k_G} = \frac{\sqrt{\varepsilon_0 d}}{\lambda} = \frac{d}{\lambda} \quad . \tag{5.4}$$

The complete expressions are given in Appendix D, whereas (5.3) represents an order-of-magnitude estimate.

The result (5.3) is interpreted in the following way: The fact that there are two regimes, crudely defined by $\lambda \ll d$ and $\lambda \gg d$, can be understood in terms of the electrons' relative response to an incident field at the top of the peaks and the bottom of the troughs. When $\lambda \gg d$ ($r \ll 1$), the electrons at the peaks' tops respond poorly by comparison to the electrons at the bottom of the troughs, simply because the former are confined to the metallic fingers of the grating. On the other hand, when $\lambda \ll d$ ($r \gg 1$), it is obvious that the response of the electrons at the peaks' top is impeded to a much lesser degree by the boundaries of the grating's fingers, while the electrons at the troughs' bottoms respond in about the same manner as in the $\lambda \gg d$ regime. This consideration implies that R(T/B) is smaller for $\lambda \gg d$ than for $\lambda \ll d$, which is born out by (3.3). The fact that in both regimes $R(T/B) \sim \beta^{-1} \ll 1$ is in keeping with the above picture: Since the grating is deep, for normal incidence it is always easier for the electrons to respond when they are located at the bottoms of the troughs than when they are

at the tops of the peaks. Note that these considerations do not depend on g, since they pertain to relative magnitude. It is interesting to notice that the same trends are present in numerical studies of shallow-gratings.[10]

6. Discussion and Summary

The main message of this work is that for the very deep sinusoidal grating limit ($\beta >>> 1$), the physics simplifies considerably: By introducing a sequence of reasonable approximations, the problem of inverting the Fresnel matrix (2.6) of order β has been reduced to the calculation of eight matrix elements (3.10). The simplicity of the outcome is in keeping with a related study of the surface-plasmon dispersion for an infinite stack of metallic thin films.[9]

With regard to the surface-plasmon dispersion relation, we find two bands, separated by a frequency band gap given by $\Delta\omega/\omega_p \approx 0.2$. These two bands represent two classes of localized SP excitations: Those for which the fields are maximized in the troughs and those where the fields are maximized inside the peaks. The latter class of modes correspond to the upper band since they represent an enhanced oscillation of the electrons. This interpretation is in keeping with the interpretation of dispersion branch pairs already observed for shallow gratings. It is also consistent with the analogy of the two-adjacent-band structure of electrons moving in a periodic potential.[12] With regard to the local field enhancement distribution, we find that the field at the bottom of the troughs is always larger than at the tops of the peaks. However, the relative magnitude of the "top/bottom" enhancement exhibits different behavior in the $\lambda >> d$ and $\lambda << d$ regimes. The existence of these regimes reflect primarily the response of the electrons at the

peaks' tops. The electrons there are restricted in their motion by the grating's boundary, and therefore respond poorly when $\lambda >> d$ and much better when $\lambda << d$.

The simple outcome of this study will hopefully stimulate further studies in the same vein. To clarify to what degree the specifics of our results do not depend on an artifact of the approximations, it would be desirable to attempt some refinements, e.g., the straight inversion of the quasi-separable approximation (3.1) or (3.2). Another possibility is to carry out large-scale exact calculations of the SG using the dressed Rayleigh expansion as described in Section 2.[3] In particular, it is interesting to substantiate the quantitative values we obtain for the width and gap of the SP bands [Eq. (4.4) and (4.5)]. These results hopefully will generate interest also for corresponding experimental work.

Acknowledgments

We are grateful to A. C. Beri for his assistance in preparing the figures and to J. Rouse, R. Ferron and L. W. Edwards for their typing of the manuscript. This work has been supported by the Office of Naval Research and the Air Force Office of Scientific Research (AFSC), United States Air Force, under Contract F49620-86-C-009. The United States Government is authorized to distribute reprints notwithstanding any copyright notation thereon.

Appendix A: Plasmon Dispersion Relation for a Shallow Grating Surface

To highlight the particular features of the $\beta << 1$ regime and to appreciate the role of the various factors in (2.6), we analyze here the shallow grating ($\beta << 1$) SP dispersion relation. The results are not new,[5,7,8] yet they are obtained here in a direct and transparent manner.

Consider first the case of a flat surface, i.e., $g = 0$ in the notation of Fig. 1. Since[14] $J_\nu(z=0) = \delta_{\nu,0}$, Eq. (2.6) yields $m=\ell$ and the matrix $\underline{M}$ is diagonal. Consequently, for the determinant of $\underline{M}$ to vanish, Eq. (4.1), one or more of the diagonal elements must vanish. Hence, the dispersion relation reads

$$W_0(\ell)W_1(\ell) + k_\ell^2 = 0 \qquad (A.1)$$

or, by inserting the definitions (2.3), (A.1) yields

$$k_\ell^2 = k^2 \frac{\varepsilon_0\varepsilon_1}{\varepsilon_0+\varepsilon_1} . \qquad (A.2)$$

For a flat surface $d \to \infty$, i.e. $k_G=0$, so that $k_\ell \to k$ and (A.2) is the well-known dispersion relation.[7,8] Thus the numerator in (2.6) involving $W_0(\ell)W_1(m) + k_\ell k_m$ entails the retardation effects, namely, that the SP dispersion relation cannot cross the boundaries of the light cone.

Consider now the case of a very shallow grating, i.e., g is finite yet $\beta = gk_G << 1$. Here the argument of the Bessel function factor is small, yet finite. Therefore, since[14]

$$\lim_{z\to 0} J_n(z) \simeq \left(\frac{z}{\nu}\right)^n \text{ for } \nu \neq 0$$

$$\simeq 1 \text{ for } \nu = 0 \qquad (A.3)$$

to first order in β, the only non-diagonal terms that contribute are when $|m-\ell| \leq 1$. Thus, $\underline{M}$ is tri-diagonal, with a dominating diagonal and

the two first-off-diagonal of order β. The $\beta = 0$ and $\beta \ll 1$ examples discussed so far clearly indicate that the Bessel function factor in (2.6) determines the amount of mixing of the m and ℓ Bragg reflections. The non-vanishing denominator of (2.6) affects only the normalization and the fall-off in m,ℓ rate of $M_{m,\ell}$.

To determine the conditions for (4.1) to hold when $\beta \ll 1$ is no simple task in general. However, for special $(k,k_{\parallel})$ combinations the problem can be easily solved. Let us thus consider, in particular, the boundary of the first Brillouin zone $k_{\parallel} = k_G/2$ and the crossing of the $\ell = 0$ and $\ell = -1$ dispersion curves given by (A.2). If there were not off-diagonal terms in $\underline{M}$, the crossing of the curves at $k_{\parallel} = k_G/2$ would define a $(k,k_{\parallel})$ point for which (4.1) is satisfied. For finite g, however, the two relevant off-diagonal elements $M_{0,-1}$ and $M_{-1,0}$ change the eigenvalues of $\underline{M}$. The condition for the perturbed eigenvalues of $\underline{M}$ to vanish [so that (4.1) is satisfied] is therefore that the corresponding determinant vanishes:

$$\left| \begin{array}{cc} M_{00} & M_{0,-1} \\ M_{-1,0} & M_{-1,-1} \end{array} \right| = 0 \qquad k_{\parallel} = k_G/2 \quad , \quad \beta \ll 1 \tag{A.4}$$

Eq. (A.4) is an equation for k which has two solutions, whose difference is the band gap. This equation can be easily solved provided that at the Brillioun zone boundary ($k_{\parallel} = k_G/2$) we are allowed to neglect retardations, i.e., $k_G \gg k(0), |k(1)|$. In this case, $W_0(0) \sim W_1(-1) \sim W_0(0) \sim W_0(-1) \sim ik_G/2$, and some simple algebra gives the gap frequency $\Delta\omega$ as[7]

$$\frac{\Delta\omega}{\omega_p} = \frac{\pi}{\sqrt{2}} \frac{g}{d} \quad . \tag{A.5}$$

Appendix B: Separable Approximation for the Bessel Function Factor in (2.6)

We derive a separable approximation to the Bessel functin factor in the matrix $\underline{M}$:

$$B_{m,\ell} = J_{m-\ell}[g(W_0(\ell)-W_1|m))]$$

$$\simeq J_{m-\ell}|i\beta(|\ell|-|m|)] \qquad (B.1)$$

which is valid for $\beta >> 1$ and $|\ell|,|m| >> 1$. The second line in (B.1) follows from (4.6). We first analyze (B.1) by considering separately the pertinent asymptotic domains and then introduce a simplifying separable expression.

When $1 << |\ell-m| <<< \beta,,$ the argument of the Bessel function (B.1) is much larger than its order. Correspondingly, the leading asymptotic term is

$$J_n(z) \simeq (\frac{2}{\pi z})^{1/2} \cos[z-(\frac{\nu}{2}+\frac{\pi}{4})]$$

$$\nu = m-\ell,\ z = i\beta(|\ell|-|m|) \simeq g[W_0(\ell)-W_1(m)] \ . \qquad (B.2)$$

When $\beta \sim |\ell-m|$, the argument of the Bessel function (B.1) and its order are large and proportional each other. The asymptotic expression in this regime is[14]

$$J_\nu(\nu z) \simeq \frac{1}{\sqrt{2\pi\nu}} \frac{1}{[1-z^2]^{1/4}} e^{\nu\Psi(z)} + \mathcal{O}(\nu^{-3/2})$$

$$\Psi(z) = \sqrt{1-z^2} + \ell n[z/(1+\sqrt{1+z^2})] \ . \qquad (B.3)$$

for $|\arg z| < \pi$, $\nu \to \infty$

To apply (B.3) to (B.1), we consider separately the three possible subdomains: (a) $\ell,m > 0$ (b) $\ell,m < 0$, (c) $|\ell| >> 1$, $|m| >> 1$ and m,ℓ of opposite signs. Using[14] $J_n(z) = (-1)^n J_n(z)$ and $J_n(-z) = (-1)^n J_n(z)$, a simple a sis gives

$$B^{\pm}_{m,\ell} = e^{\mp \frac{i\pi}{2}|\ell-m|} \frac{1}{\sqrt{2\pi|\ell-m|}} \frac{1}{[1+\beta^2]^{1/4}} e^{|\ell-m|\eta(\beta)}$$

$$\eta|\beta) = \sqrt{1+\beta^2} + \ell n[\beta/(1+\sqrt{1+\beta^2})] \qquad (B.4)$$

where B^+ refers to domain (a) and B^- to domain (b). When ℓ and m have different signs [domain (c)], the argument of the Bessel function (B.1) is much smaller than its order, and hence the corresponding asymptotic expression is[14]

$$J_\nu(z) \simeq \frac{1}{\sqrt{2\pi\nu}} \left(\frac{ez}{2\nu}\right)^\nu, \quad \nu = m-\ell, \; z = i\beta(|\ell|-|m|) \; . \qquad (B.5)$$

Consequently, $z/\nu \sim \beta\,|(\ell+m)/(\ell-m)| \ll 1$ and hence $B_{m,\ell} \approx 0$ for most of the m,ℓ combinations.

Given (B.2)-(B.5), the approximation

$$J_{m-\ell}[g(W_0(\ell)-W_1(m))] \simeq \sqrt{\frac{k_G}{2\pi}} \frac{1}{(1+\beta^2)^{1/4}} \frac{1}{[W_0(\ell)-W_1(m)]^{1/2}} \{\exp(i\phi) + \exp(-i\phi)\}$$

$$\phi = \frac{\eta(\beta)}{k_G}[W_0(\ell)-W_1(m)] - [\frac{(m-\ell)}{2}+\frac{1}{4}]\pi \qquad (B.6)$$

unifies all relevant domains.

Appendix C: Reduced Auxiliary Matrix $\underline{A}$

We calculate some and estimate the remaining matrix elements of the auxiliary matrix $\underline{A}$ defined by

$$A_{i,j} = \sum_{\ell=-\infty}^{\infty} b_i(\ell)a_j(\ell) \ , \quad i,j = 1,..4 \tag{C.1}$$

where, from (3.1) and (3.3),

$$\begin{aligned}
a_1(m) &= W_1(m)\ \exp[i(W_1(m)(g-\eta(\beta)/k_G)-\tfrac{\pi}{4})] \\
b_2(\ell) &= CW_0(\ell)\ \exp[i(W_0(\ell)(g+\eta(\beta)/k_G))] \\
a_2(m) &= W_1(m)\ \exp[i(W_1(m)(g+\eta(\beta)/k_G) + \pi m + \tfrac{\pi}{4})] \\
b_2(\ell) &= CW_0(\ell)\ \exp[i(W_0(\ell)(g-\eta(\beta)|k_G) - \pi\ell)] \\
a_3(m) &= k_m\ \exp[i(W_1(m)(g-\eta(\beta)/k_G) - \tfrac{\pi}{4})] \\
b_3(\ell) &= Ck_\ell\ \exp[i(W_0(\ell)(g+\eta(\beta)/k_G))] \\
a_4(m) &= k_m\ \exp[i(W_1(m)(g+\eta(\beta)/k_G) + \pi m + \tfrac{\pi}{4})] \\
b_4(\ell) &= Ck_\ell\ \exp[i(W_0(\ell)(g-\eta(\beta)/k_G) - \pi\ell)]
\end{aligned} \tag{C.2}$$

and C is defined in (3.3). Note that in (C.1) all the ℓ-dependence enters via the combintion $k_\ell = k_{||} + \ell k_G$ [see (C.2)]. Hence, the summation in (C.1) can be evaluated by using the Poisson formula:[15]

$$\sum_{\ell=-\infty}^{\infty} G(y+\ell\Delta) = \frac{1}{\Delta} \sum_{m=-\infty}^{\infty} g(2\pi n/\Delta)\ e^{-2\pi i n y/\Delta} \quad g(t) = \int_{-\infty}^{\infty} du\ G(u)e^{itu} \tag{C.3}$$

with the identifictaions $y \to k_{||}$, $\Delta \to k_G$ and $u \to k_\ell$. Furthermore, since for most terms in (C.1) $|\ell| >> 1$, it is justified to evaluate $A_{i,j}$ using the asymptotic expression of $W_j(\ell)$, Eq. (4.6). Keeping the leading term in (4.6) is not sufficient since all references to k(j) enter in the second term. It is therefore the first small connection to $A_{i,j}$, beyond the leading term, that carries all the physics.

Inserting (4.6) into (C.2), it is easily seen that all Fourier transforms g(u) mandated by (C.3) take the form

$$g_{ij}(t) = \int_{-\infty}^{\infty} dk_\ell \; b_i(k_\ell) a_j(k_\ell) e^{ik_\ell t} = \int_{-\infty}^{\infty} dk_\ell \; F_n(k_\ell) e^{i[f_\eta(k_\eta)+k_\ell t]_\ell}$$

for: $i,j = 1,\ldots 4$; $n = 1,\ldots 4$ and $\eta = \alpha,\beta,\gamma,\delta$. (C.4)

where

$$F_1(k_\ell) = W_0(\ell)\, W_1(\ell) \simeq C\{-k_\ell^2 + \tfrac{1}{2}[k^2(0)+k^2(1)]\}$$

$$F_2(k_\ell) = C\{-ik_\ell|k_\ell| + \tfrac{i}{2}k^2(0)\,\mathrm{sgn}(k_\ell)\}$$

$$F_3(k_\ell) = C\{-ik_\ell|k_\ell| + \tfrac{i}{2}\,k^2(1)\,\mathrm{sgn}(k_\ell)\}$$

$$F_4(k_\ell) = C\{k_\ell^2\} \qquad (C.5)$$

and

$$f_\alpha = +\tfrac{\pi}{4} + W_0(\ell)(g-\eta(\beta)/k_G + W_1(\ell)[g+\eta(\beta)/k_G]$$

$$\simeq \tfrac{\pi}{4} + 2ig|k_\ell| - igk^2(1)\frac{1}{|k_\ell|}$$

$$f_\beta = -\tfrac{\pi}{4} + W_0(\ell)[g+\eta(\beta)/k_G] + W_1(\ell)[g-\eta(\beta)/k_G]$$

$$\simeq -\tfrac{\pi}{4} + 2ig|k_\ell| - igk^2(0)\,\frac{1}{|k_\ell|}$$

$$f_\gamma = \tfrac{\pi}{4} + W_0(\ell)[g+\eta(\beta)/k_G] + W_1(\ell)[g+\eta(\beta)] + \pi\ell$$

$$\simeq \tfrac{\pi}{4} - \pi k_{||}/k_G + \pi k_\ell/k_G + 4ig|k_\ell| - ig[k^2(0)+k^2(1)]/|k_\ell|$$

$$f_\delta = -\tfrac{\pi}{4} + W_0(\ell)[g-\eta(\beta)/k_G] + W_1(\ell)[g-\eta(\beta)|k_G] - \pi\ell$$

$$\simeq -\tfrac{\pi}{4} + \frac{\pi k_{||}}{k_G} - \frac{\pi k_\ell}{k_G} + \frac{i}{\beta k_G}\,|k_\ell| - \frac{i[k^2(0)+k^2(1)]}{4\beta k_G}\;\frac{1}{|k_\ell|} \; . \qquad (C.6)$$

The sixteen Fourier transforms $g_{i,j}(t)$ [Eq.(C.4)] are obtained from all combinations of the F_m and the f_η. The explicit correspondence in (Table 1) is

$$f_\alpha \text{ with } A_{2,2},\ A_{2,4},\ A_{4,2},\ A_{4,4}$$
$$f_\beta \text{ with } A_{1,1},\ A_{1,3},\ A_{3,1},\ A_{3,3}$$
$$f_\gamma \text{ with } A_{1,2},\ A_{1,4},\ A_{3,2},\ A_{3,4}$$
$$f_\delta \text{ with } A_{2,1},\ A_{2,3},\ A_{4,1},\ A_{4,3} \qquad \text{(C.7)}$$

The procedure of calculating $A_{i,j}$ is now clear. We first evaluate the transforms (C.4) for all t-values mandated by the Poisson formula (C.3), and then sum the contributions. As we now show, these two operations can be carried out in closed form. An important bonus of having analytical expressions is the possibility to identify the dominating matrix elements of $\underline{A}$.

Combining (C.5) and (C.6) with (4.6) implies that all integrals (C.4) are combinations of[16]

$$\int_0^\infty dx\ x^{\nu-1}\ \exp[\tfrac{i\mu}{2}\ (x - \frac{\gamma^2}{x})] = 2\gamma^\nu\ e^{\frac{i\pi\nu}{2}}\ K_{-\nu}(\gamma\mu) \qquad \text{(case I)}$$

$$\int_0^\infty dx\ x^{\nu-1}\ \exp[\tfrac{i\mu}{2}\ (x + \frac{\gamma^2}{x})] = i\pi\ \gamma^\nu\ e^{\frac{i\pi\nu}{2}}\ H^{(1)}_{-\nu}(\gamma\mu) \qquad \text{(case II)}$$

$$\text{for } Im(\mu) > 0,\quad Im(\gamma^2\mu) > 0,\quad \text{any } \nu \qquad \text{(C.8)}$$

where K_ν and $H^{(1)}_\nu$ denote the modified Bessel and Hankel functions of the first kind of order ν, respectively. As will become clear shortly, we shall need only the asymptotic or nearthe origin behavior the Bessel function, given by[14]

$$K_{-\nu}(z) \sim [\frac{\pi}{2z}]^{1/2}\ e^{-z}$$
$$H^{(1)}_{-\nu}(z) \sim [\frac{2}{\pi z}]^{1/2}\ e^{i[z + \frac{\pi\nu}{2} - \frac{\pi}{4}]}$$
$$\text{for } |z| \to \infty \qquad \text{(C.9.a)}$$

and

$$K_{-\nu}(z) \simeq \frac{1}{2}\,\Gamma(\nu)\,(\frac{z}{2})^{-\nu}$$

$$H^{(1)}_{-\nu}(z) \simeq -\frac{1}{\pi}\,\Gamma(\nu)\,e^{i\pi\nu}(\frac{z}{2})^{-\nu}$$

$$\text{for } |z| \to 0 \quad . \qquad \text{(C.9.b)}$$

Before proceeding further, we mention that the conditions attached to (C.8), i.e., $\mathrm{Im}(\mu) > 0$, etc. are always fulfilled. Also because the k_ℓ-integration in (C.3) is over the whole k_ℓ-axis while in (C.8) it runs over only half the axis, we subdivide the k_ℓ-integration into $-\infty \leq k_\ell \leq 0$ and $0 \leq k_\ell \leq \infty$. The respective contributions are denoted by the "-" and "+" superscripts in (C.10).

By virtue of (C.8) and (C.9), we obtain now an estimate of the magnitude of $g_{i,j}(t)$ (and therefore of the t-summed expression) by considering the "$\gamma\mu$" argument in (C.8). This factor determines the dominating exponential or power in the expression for $g_{i,j}(t)$. Constant phases, etc., are omitted in (C.10), but are included in the final expressions. Straightforward algebra based on (C.3) and (C.6) gives

$$\gamma^{\pm}_{\alpha} = [-\frac{ik^2(1)}{2ig \pm t}]^{1/2} \quad , \qquad \text{(Case II)}$$

$$\gamma^{\pm}_{\alpha}\,\mu^{\pm}_{\alpha} = 2[(2ig \pm t)(-ik^2(1)g)]^{1/2}$$

$$\simeq 2[2g^2k^2(1)]^{1/2}(1 \pm \frac{it}{4g}) \qquad \text{for } g \gg t$$

$$\simeq 2[itgk^2(1)]^{1/2}(1 \pm \frac{ig}{t}) \qquad \text{for } g \ll t$$

$$\gamma^{\pm}_{\beta} = [+\frac{ik^2(0)}{2ig\pm t}]^{1/2} \quad , \quad \text{(Case I)}$$

$$\gamma^{\pm}_{\beta}\mu^{\pm}_{\beta} = 2[(2ig\pm t)(ik^2(0)g)]^{1/2}$$

$$\simeq 2[-2g^2k^2(0)]^{1/2}(1 \mp \frac{it}{4g}) \quad \text{for } g >> t$$

$$= 2[itgk^2(0)]^{1/2}\ (1 \pm \frac{ig}{t}) \quad \text{for } g << t$$

$$\gamma_\gamma^\pm = \left[-\frac{ig(k^2(0)+k^2(1)}{4ig \pm t \pm \pi/k_G}\right]^{1/2} \quad \text{(Case II)} \quad \text{for } k < k_p/\sqrt{2}$$

$$\gamma_\gamma^\pm = \left[+\frac{ig(k^2(0)+k^2(1)}{4ig \pm t \pm \pi/k_G}\right]^{1/2} \quad \text{(Case I)} \quad \text{for } k > k_p/\sqrt{2}$$

$$\gamma_\gamma^\pm\mu_\gamma^\pm = 2[(4ig \pm t \pm \pi/k_G)(-ig(k^2(0) + k^2(1))]^{1/2} \text{ for } k < k_p/\sqrt{2}$$

$$= 2[4g^2(k^2(0) + k^2(0)]^{1/2}[1 \mp \frac{1}{8g}(t+\pi/k_G] \quad \text{for } g >> t$$

$$= 2[g(t+\pi/k_G)i(k^2(0) + k^2(1))]^{1/2}[1 \pm \frac{4ig}{t+\pi/k_G}] \quad \text{for } g << t$$

$$\gamma_\gamma^\pm\mu_\gamma^\pm = 2[(4ig \pm t \pm \pi/k_G)(+ig(k^2(0) - k^2(1)))]^{1/2} \text{ for } k_0 > k_p/\sqrt{2}$$

$$= 2[-4g^2(k^2(0) + k^2(1))]^{1/2}[1 \mp \frac{1}{8g}(t+\pi/k_G)] \text{ for } g >> t$$

$$= 2[g(t+\pi/k_G)i(k^2(0)+k^2(1))]^{1/2}[1 \mp \frac{4ig}{t+\pi/k_G}] \quad \text{for } g << t$$

$$\gamma_\delta^\pm = \left[-\frac{i(k^2(0) + k^2(1))}{4\beta k_G[\frac{i}{\beta k_G} \pm t \mp \pi/k_G]}\right]^{1/2} \text{(Case II) for } k < k_p/\sqrt{2}$$

$$= \left[+\frac{i^2k\ (0) +^2k\ (1))}{4_\beta k_G[\frac{1}{\beta k_G} \pm t \mp \pi/k_G]}\right]^{1/2} \text{(Case I) for } k > k_p\sqrt{2}$$

$$\gamma_\delta^\pm\mu_\delta^\pm = 2[(\frac{i}{\beta k_G} \pm t \mp \pi/k_G)(-\frac{i}{4\beta k_G}(k^2(0) + k^2(1)))]^{1/2} \text{ for } k_0 < k_p\sqrt{2}$$

$$= 2[(\frac{i}{\beta k_G} \pm t \mp \frac{\pi}{k_G})(+\frac{i}{4\beta k_G}(k^2(0) + k^2(1)))]^{1/2} \text{ for } k_0 > k_p/\sqrt{2}$$

for all t (C.10)

where $k_p = \omega_p/c$ and where the square roots in (C.10) and throughout [Eq. (2.3)] are chosen so that the real or imaginary parts are positive. We have also used in (C.10), and in the rest of this Appendix, $\epsilon_0=1$, and the notation "Cases I and II" are defined in (C.8).

Expressions (C.10) yield a quick order-of-magnitude estimate for $g_{i,j}(t)$. Consider first the $g \gg t$ regime. Since $gk(0) \sim gk(1) \sim gk_p \sim \beta \gg 1$, the elements belonging to classes α, β and γ call for the asymptotic limit (C.9.a), while those of class δ call for the limit (C.9.b). Therefore, the leading t-independent terms in (C.10) yield the following dominating exponents in $g_{i,j}(t)$ (Table 1):

$$\text{class } \alpha \sim e^{2i[2g^2k^2(1)]^{1/2}}$$

$$\text{class } \beta \sim e^{-2[-2g^2k^2(0)]^{1/2}}$$

$$\text{class } \gamma \sim e^{2i[4g^2(k^2(0)+k^2(1))]^{1/2}} \quad \text{for } k \leq k_p/\sqrt{2}$$

$$\sim e^{-2[-4g^2(k^2(0)+k^2(1))]^{1/2}} \quad \text{for } k \geq k_p/\sqrt{2}$$

$$\text{class } \delta \sim 1$$

$$\text{for } g \gg t \ . \qquad \text{(C.11)}$$

The symbol "1" is the class-δ entry indicates that no exponential factors appear, only powers. Estimates (C.11) imply that as $\beta \to \infty$, the class-α elements are always the smallest [$k^2(1) < 0$, always]. The class-γ *elements are larger than the class-α elements by a factor* $\exp[2i[4g^2k^2(1)]^{1/2}k^2(0)/k^2(1)] \gg 1$ for $k < k_p/\sqrt{2}$, and by yet a larger factor when $k > k_p/\sqrt{2}$. It is therefore justified to discard (set to zero) the class-α elements for the $g \gg t$ regime.

Consider now the complementary $g \ll t$ regime. Considerations similar to those above yield

$$\text{class } \alpha \sim e^{2i[itgk^2(1)]^{1/2}}$$

$$\text{class } \beta \sim e^{-2[itgk^2(0)]^{1/2}}$$

$$\text{class } \delta \sim e^{2i[itg(k^2 0) + k^2(0))]^{1/2}} \quad \text{for } k \leq k_p/\sqrt{2}$$

$$\sim e^{-2[itg(k^2(0) + k^2(1))]^{1/2}} \quad \text{for } k \geq k_p/\sqrt{2}$$

$$\text{class } \delta \sim 1$$

$$\text{for } g \ll t \,. \tag{C.12}$$

Since the real and imaginary parts of the square root are always chosen to be positive, (C.12) clearly indicates that the elements belonging to classes α, β and γ are <u>exponentially</u> small, while the class-δ elements are of the order 1 (i.e., fall off as an inverse power). Therefore, in conjunction with the Poisson sum (C.3), there is a sharp cutoff in the u-summation for the $g_{i,j}(t)$ pertaining to classes α, β and γ, whereas for the class-δ element it is necessary to sum all the way to infinity. The cutoff L (in the u-summation) occurs [from (C.10)] when $2\pi L/k_G = t \sim 2g$ or $L \approx \beta/\pi \ggg 1$. It is sharp in the sense that over a range $\Delta nL \ll 1$ the n-dependent contributions diminish as $e^{-\sqrt{\beta}}$.

The asymptotic ($\beta \gg 1$) vanishing by the class-α elements implies that in the evalution of $\underline{A}^{-1}$ only the eight elements of clases γ and δ contribute[17]. We therefore turn now to the calculation of these entries for a fixed t and then consider the summation mandated by the Poisson formula (C.3). Straightforward algebra gives for the class-γ elements

$$g_{1,2}(t) = P_{\gtrless}^{\gtrless}(g,k_{\parallel})\left[\tfrac{3}{4}(k^2(0) + k^2(1)\right] \cos[\nu_{\gtrless}(t)]$$

$$g_{3,4}(t) = P_{\gtrless}^{\gtrless}(g,k_{\parallel})\left[\tfrac{1}{4}(k^2(0) + k^2(1)\right] \cos[\nu_{\gtrless}(t)]$$

$$g_{1,4}(t) = P_{\gtrless}^{\gtrless}(g,k_{\parallel})\left[\tfrac{1}{4}(3k^2(0) + k^2(1))\right] i \sin[\nu_{\gtrless}(t)]$$

$$g_{3,2}(t) = P_{\gtrless}^{\gtrless}(g,k_{\parallel}) \left[\tfrac{1}{4}(k^2(0) + 3k^2(1))\right] i \sin[\nu_{\gtrless}(t)] \qquad (C.13)$$

where the labels > and < refer to the domains where $k \geq k_p/\sqrt{2}$ or $k \leq k_p/\sqrt{2}$, respectively, and

$$P_{\gamma}^{>}(g,k_{\parallel}) = \frac{2C}{k_G}\left[\frac{k^2(0)+k^2(1)}{4}\right]\left[\frac{\pi \exp(i\pi)}{[-4g^2(k^2(0)+k^2(1))]^{1/2}}\right]^{1/2}$$

$$\times \exp[i\pi(\tfrac{1}{4} - k_{\parallel}/k_G)] \exp[-2[-4g^2(k^2(0)+k^2(1))]^{1/2}]$$

$$\gamma_{>}(t) = 2[-4g^2(k^2(0)+k^2(1))]^{1/2} \left(\frac{1}{4g}\right)(t + \pi/k_G)$$

$$P_{\gamma}^{<}(g,k_{\parallel}) = \frac{2iC}{k_G}\left[-\frac{k^2(0)+k^2(1)}{4}\right]^{1/2}\left[\frac{\pi \exp(-i\pi/2)}{[4g^2(k^2(0)+k^2(1))]^{1/2}}\right]^{1/2}$$

$$\times \exp[i\pi(\tfrac{1}{4} - k_{\parallel}/k_G)] \exp[2i[4g^2(k^2(0)+k^2(1))]^{1/2}]$$

$$\nu_{<}(t) = 2i[4g^2(k^2(0)+k^2(1))]^{1/2}\left(\frac{1}{4g}\right)(t + \pi/k_G). \qquad (C.14)$$

Note that $\gamma_{\gtrless}(t)$ do not depend on g! Similarly, the class-3 elements

$$g_{2,1}(t) = P_\delta(k_{||}) \left[2e^{3\pi i/2}(I_3^-(g,t) + I_3^+(g,t)) \right.$$

$$\left. + \frac{1}{2}(k^2(0) + k^2(1))\, e^{i\pi/2}(I_1^-(g,t) + I_1^+(g,t))\right]$$

$$g_{2,3}(t) = P_\delta(k_{||}) \left[2e^{3\pi i/2}(-i)(I_3(\bar{g},t) - I_3^+(g,t)) \right.$$

$$\left. + \frac{i}{2}\, k^2(0)\, e^{i\pi/2}(I_1^-(g,t) - I_1^+(g,t))\right]$$

$$g_{4,1}(t) = P_\delta(k\ ) \left[-2i\, e^{3\pi i/2}(I_3^-(g,t) - I_3^+/g,t)) \right.$$

$$\left. + \frac{i}{2}\, k^2(1)\, e^{i\pi/2}(I_1^-(g,t) - I_1^+(g,t))\right]$$

$$g_{4,3}(t) = P_\delta(k\ )\, 2e^{3\pi i/2}(I_3^-(g,t) + I_3^+(g,t)) \ , \qquad \text{(C.15)}$$

where

$$P_\delta(k\ ) = C \exp\left[i(-\frac{\pi}{4} + \pi k_{||}/k_G)\right]$$

$$I_n^\pm(g,t) = \left[\frac{i}{\beta k_G} \pm t \mp \pi/k_G\right]^n \ . \qquad \text{(C.16)}$$

Expressions (C.15) and (C.16) are valid for the whole $k \leq k_p$ domains.

The last step is to perform the t-summation implied by (C.3). As pointed out before, for the class-δ elements (C.16), there is a sharp cutoff at $t = 2\pi n/k_G - 2g$, whereas for the class-δ elements (C.18) all values of $t = 2\pi n/k_G$ must be summed. The summations pertaining to (C.13) and (C.15) are simply caried out by using the identities[18]

$$I_c(\alpha,\gamma) = \sum_{m=-L}^{L} e^{-i\gamma n} \cos[\alpha(n+1/2)]$$

$$= \frac{1}{2} e^{+i\gamma/2} \left[\frac{\sin[L(\alpha+\gamma)]}{\sin(\frac{\alpha+\gamma}{2})} + \frac{\sin[L(\alpha-\gamma)]}{\sin(\frac{\alpha-\gamma}{2})}\right]$$

$$I_s(\alpha,\gamma) = \sum_{n=-L}^{L} e^{-i\gamma W} \sin[\alpha(n+1/2)]$$

$$= \frac{i}{2} e^{+i\gamma/2} \left[\frac{\sin[L(\alpha+\gamma)]}{\sin(\frac{\alpha+\gamma}{2})} - \frac{\sin[L(\alpha-\gamma)]}{\sin(\frac{\alpha-\gamma}{2})}\right]$$

$$I_1(\alpha,\gamma) = \sum_{n=-\infty}^{\infty} e^{-i\gamma n} \frac{1}{\alpha+n}$$

$$= + \frac{\pi e^{+i\alpha\gamma}}{\sin(\alpha\pi)}$$

$$I_3(\alpha,\gamma) = \frac{1}{2} \frac{d^2}{d\alpha^2} I_1(\alpha,\gamma) \quad . \qquad \text{(C.17)}$$

Using (C.17) in (C.3) gives for the class-γ matrix elements

$$A_{1,2} = P_{\alpha}^{\gtrless}(g,k_{\parallel}) \left[\tfrac{3}{4}(k^2(0)+k^2(1))\right] I_c(\alpha_{\gtrless},\gamma)$$

$$A_{3,4} = P_{\gamma}^{\gtrless}(g,k_{\parallel}) \left[\tfrac{1}{4}(k^2(0)+k^2(1))\right] I_c(\alpha_{\gtrless},\gamma)$$

$$A_{1,4} = P_{\gamma}^{\gtrless}(g,k_{\parallel}) \left[\tfrac{1}{4}(3k^2(0)+k^2(1)\right] i\ I_s(\alpha_{\gtrless},\gamma)$$

$$A_{3,2} = P_{\gamma}^{\gtrless}(g,k_{\parallel}) \left[\tfrac{1}{4}(k^2(0)+3k^2(1)\right] i\ I_s(\alpha_{\gtrless},\gamma) \ ,$$

where

$$\alpha_< = i[k^2(0)+k^2(1)]^{1/2}\pi/k_G \quad \text{for } k < k_p/\sqrt{2}$$

$$\alpha_> = [-(k^2(0)+k^2(1)]^{1/2}\pi/k_G \quad \text{for } k > k_p/\sqrt{2} \tag{C.18}$$

and

$$\gamma = +2\pi k_{\parallel}/k_G \, . \tag{C.19}$$

For the class-δ matrix elements we obtain

$$A_{2,1} = 0 \quad [\text{of order } (1/\beta)])$$

$$A_{2,3} = \frac{1}{2} P_\delta(k) \, e^{-i\gamma/2}\{ 2(\pi^2+\gamma^2)(\frac{k_G}{2\pi})^2 - k^2(0)\}$$

$$A_{4,1} = \frac{1}{2} P_\delta(k) \, e^{-i\gamma/2}\{2(\pi^2+\gamma^2)(\frac{k_G}{2\pi})^2 - k^2(1)\}$$

$$A_{4,3} = 0 \quad [\text{of order } \mathcal{O}(1/\beta)] \tag{C.20}$$

In evaluating (C.20) we used $\alpha = -1/2 + \mathcal{O}(1/\beta) \approx -0.5$ in $I_1(\alpha,\gamma)$ and $I_3(\alpha,\gamma)$ of Eq. (C.17), and γ is defined in (C.19). Note that $A_{4,1}$ never vanishes and $A_{2,3}$ vanishes along a curve <u>within</u> the light cone $k(0) = k_{\parallel}$.

Appendix D: Local Field Enhancement

Our starting point is the projection of the slow component in the field, $\vec{E}_s(X,Z)$ [EQ. (5.1)], along a vector $\hat{v}$, which is either $\hat{x}$ or $\hat{z}$. From (5.1), (3.16) and (C.20) one observes

$$\hat{v}\cdot\vec{E}_{\Delta}(x,z) = \frac{1}{D}\Big\{\sum_{\ell=-\infty}^{\infty} X_\ell \mu(\ell) - \frac{1}{A_{4,1}}\Big[\sum_\ell X_\ell a_1(\ell)\Big]\Big[\sum_\ell X_\ell a_1(\ell)\Big]\Big[\sum_\ell b_4(\ell)\mu(\ell)\Big]$$

$$- \frac{1}{A_{2,3}}\Big[\sum_\ell X_\ell a_3(\ell)\Big]\Big[\sum_\ell b_2(\ell)\mu(\ell)\Big]\Big\}$$

$$X_\ell = \hat{v}\cdot\hat{p}_{0,+}(\ell)\, e^{i[k_\ell x + W_0(\ell)z]} \quad . \tag{D.1}$$

For $\beta >> 1$ and normal incidence ($k_{||} = 0$), the entries to (D.1) are [Eqs. (2.6), (3.3), (4.16) and (C.2)]

$$\mu(\ell) = -\frac{ik(0)}{\beta^{1/2}}\frac{1}{\sqrt{2\pi}}\frac{1}{\sqrt{|\ell|}}\exp[[-|\ell|/2\beta] \qquad |\ell| >> 1$$

$$a_1(\ell) = ik_G \exp(-i\pi/4)\,|\ell|\exp[-|\ell|/2\beta]$$

$$a_3(\ell) = k_G \exp[-i\pi/4]\,\ell\exp[-|\ell|2\beta]$$

$$b_2(\ell) = C\, ik_G\,|\ell|\,(-1)^\ell \exp[-[\ell|/2\beta]$$

$$b_4(\ell) = C\, k_G \ell(-1)^\ell \exp[-|\ell|/2\beta] \quad , \tag{D.2}$$

and from (2.3) one deduces[14]

$$\mu(0) = +\, i\exp[-i/gk(0) + \pi/4]\,\frac{k(0)\,k(1)}{[k(0)+k(1)]^{3/2}}\,\frac{1}{\sqrt{2\pi g}} \quad . \tag{D.3}$$

We now specialize (D.1) to points T and B in the notation of Fig. 1. Using the definitions (2.3), one obtains

$$X_\ell(T;\hat{x}) = -\frac{W_0(\ell)}{k(0)}\exp[2iW_0(\ell)g]$$

$$= -\mathcal{O}([r]-|\ell|\exp[2ik(0)g]$$

$$X_\ell(T;\hat{z}) = \frac{k_\ell}{k(0)}\exp[2iW_0(\ell)g]$$

$$= \frac{\ell}{r}\mathcal{O}([r]-|\ell|\exp[2ik(0)g]$$

$$X_\ell(B;\hat{x}) = -\frac{W_0(\ell)}{k(0)}\exp[ik_\ell d/2] = -\frac{i}{r}|\ell|(-1)^\ell$$

$$X_\ell(B;\hat{z}) = \frac{k_\ell}{k(0)}\exp[ik_\ell d/2] = \frac{\ell}{r}(-1)^\ell \qquad (D.4)$$

where, for instance, $X_\ell(T;\hat{x})$ indicates that in (D.1) one substitutes $\hat{v} = \hat{x}$ and the coordinates of point A,

$$r = \frac{k(0)}{k_G} = \frac{\sqrt{\varepsilon_0}d}{\lambda} \quad , \qquad (D.5)$$

[r] is the integer closest to r from below, and λ is the wavelength of the incident light.

With the help of (D.2), (D.3) and (D.4), the field projections (D.1) can now be calculated in a straightforward manner. Note first that since $b_4(\ell) = -b_4(-\ell)$ and $\mu(\ell) = \mu(-\ell)$, the term is (4.1) involving $A_{4,1}$ does not contribute. The other terms give

$$\hat{x}\cdot\vec{E}_s(T) = \frac{1}{D}\left\{\sum_{\ell=\infty}^{\infty} X_\ell(T,\hat{x})\,\mu(\ell)\right\}$$

$$\hat{z}\cdot\vec{E}_s(T) = \frac{1}{D}\left\{-\frac{1}{A_{2,3}}\left[\sum_\ell X_\ell(T,\hat{z})\,a_3(\ell)\right]\left[\sum_\ell b_2(\ell)\,\mu(\ell)\right]\right\}$$

$$\hat{x}\cdot\vec{E}_s(B) = \frac{1}{D}\left\{\sum_{\ell=\infty}^{\infty} X_\ell(B,\hat{x})\,\mu(\ell)\right\}$$

$$\hat{z}\cdot\vec{E}_s(B) = \frac{1}{D}\left\{-\frac{1}{A_{2,3}}\left[\sum X_\ell(B,\hat{z})\,a_3(\ell)\right]\left[\sum b_2(\ell)\,\mu(\ell)\right]\right\} \quad , \qquad (D.6)$$

or explicitly

$$|\hat{x}\cdot\vec{E}_s(T)|^2 = \frac{1}{D^2}\frac{k^2(0)}{2\pi\beta r}\left|\frac{\sqrt{\varepsilon_0\varepsilon_1}}{(\sqrt{\varepsilon_0}+\sqrt{\varepsilon_1})^{3/2}}\right|^2 \qquad \text{for } r \ll 1$$

$$= \frac{1}{D^2}\frac{k^2(0)}{2\pi\beta} I_{T,x}^2 \qquad \text{for } r \gg 1$$

$$|\hat{z}\cdot\vec{E}_s(T)|^2 = \frac{1}{D^2}\frac{4k^2(0)}{r^2[\frac{1}{2}-r^2]^2}\frac{I_2^2 I_{T,z}^2}{2\pi\beta}$$

$$|\hat{x}\cdot\vec{E}_s(B)|^2 = \frac{1}{D^2}\frac{k^2(0)}{2\pi\beta}\frac{1}{r^2} I_{B,x}^2$$

$$|\hat{z}\cdot\vec{E}_s(B)|^2 = \frac{1}{D^2}\frac{4k^2(0)}{2\pi\beta}\frac{1}{r^2(\frac{1}{2}-r^2)^2} I_2^2 I_{B,z}^2 \qquad \text{(D.7)}$$

where

$$I_2 = \sum_{\ell=-\infty}^{\infty} \sqrt{|\ell|}\,(-1)^{\ell} \exp[-|\ell|/\beta] - \frac{1}{\sqrt{\beta}}$$

$$I_{T,x} = \sum_{|\ell|>1}^{[r]} \frac{1}{\sqrt{|\ell|}} \exp[-|\ell|/2\beta] - \sqrt{r}\,, \qquad 1 \ll r < 2\beta$$

$$I_{T,z} = \sum_{\ell=-[r]}^{[r]} \ell^2 \exp[-|\ell|/2\beta] - r^3$$

$$I_{B,x} = \sum_{\ell=-\infty}^{\infty} \sqrt{|\ell|}(-1)^{\ell} \exp[-|\ell|/2\beta] - \frac{1}{\sqrt{\beta}}$$

$$I_{B,z} = \sum_{\ell=-\infty}^{\infty} \ell^2 (-1)^{\ell} \exp[-|\ell|/2\beta] - \beta\,. \qquad \text{(D.8)}$$

We added in (D.7) an order-of-magnitude estimate for the various sums. Using (D.6), we obtain (5.3).

References

1. S.R.J. Brueck and D.J. Ehrlich, Phys. Rev. Lett. 48, 1678 (1982).

2. C. J. Chen, H. H. Gilgen and R. M. Osgood, Opt. Lett. 10, 173 (1985).

3. D. Agassi and T.F. George, Phys. Rev. B, submitted.

4. "Electromagnetic Theory of Diffraction Gratings" edited by R. Petit (Springer, New York, 1980).

5. See, for example, F. Toigo, A. Marvin, C. Celli and N.R. Hill, Phys. Rev. B 15, 5618 (1977); N. Garcia, V. Celli, N.R. Hill and N. Cabrera, Phys. Rev. B 18, 5184 (1978); N. Garcia, G. Diaz, J.J. Saenz and C. Ocal, Surf. Sci. 143, 338 (1984).

6. P. Sheng, R.S. Stepleman and P.N. Sanda, Phys. Rev. B 26, 2907 (1982); K.T. Lee and T.F. George, Phys. Rev. B 31, 5106 (1985).

7. B. Laks, D.L. Mills and A.A. Maradudin, Phys. Rev. B 23, 4965 (1981); N.E. Glass and A.A. Maradudin, Phys. Rev. B 24, 595 (1981).

8. "Surface Polaritons", edited by V.M. Agranovich and D.L. Mills (North-Holland, New York, 1982).

9. E.N. Economou, Phys. Rev. 182, 539 (1968).

10. See, for example, M. Weber and D.L. Mills, Phys. Rev. B 27, 2698 (1983); E.V. Alband, S. Daiser, G. Ertl, R. Miranda, K. Wandelt and N. Garcia, Phys. Rev. Lett. 51, 2314 (1983).

11. See, for example, M. Hutchinson, K.T. Lee, W.C. Murphy, A.C. Beri and T.F. George, in "Laser-Controlled Chemical Processing of Surfaces", edited by A.W. Johnson, D.J. Ehrlich and H.R. Schlossberg (Elsevier, New York), Mat. Res. Soc. Symp. Proc. 29, 389 (1984).

12. N.D. Ashcroft and N.D. Mermin, "Solid State Physics" (Holt, Rinehardt and Winston, New York, 1976), Chapt. 9.

13. See, for example, P.K. Aravind and H. Metiu, Surf. Sci. 124, 506 (1983).

14. M. Abramowitz and I.A. Stegun, "Handbook of Mathematical Functions" (National Bureau of Standards, Washington, D.C., 1964), Chapt. 9.

15. F. Oberhettinger, "Fourier Expansions" (Academic Press, New York, 1973), p. 5.

16. I.S. Gradshteyn and I.M. Ryzhik, "Table of Integrals, Series, and Products"' (Academic Press, New York, 1965), p. 340, relations 10 and 11.

17. See, for example, M.L. Mehta, "Elements of Matrix Theory" (Hindustan Publishing, Delhi, 1977), p. 21.

18. Ref. 16, p. 30, relations 3 and 4; ibid., p. 40, relations 5 and 6.

	1	2	3	4
1	β	γ	β	γ
2	δ	α	δ	α
3	β	γ	β	γ
4	δ	α	δ	α

Table 1: Outlay of the $A_{i,j}$ elements according to the classification defined in Eq. (C.7). The discussion in Appendix C implies that for $\beta \to \infty$, the class-α terms can be neglected in comparison to the other entries.

Figure Captions

1. Schematic display of the sinusoidal [$z = g \cos(2\pi x/d)$] grating and the notation used in this work. The incident light ($\bar{E}_{0p}$ and the energy Bragg reflection are indicated. The points "T" and "B" are those for which the local field enhancement is evaluated.
2. Display of the surface-plasmon flat bands, Eq. (4.4). The light cone is indicated left of the diagonal line, and $k_p = \omega_{p/c}$ is the volume plasma wave vector.

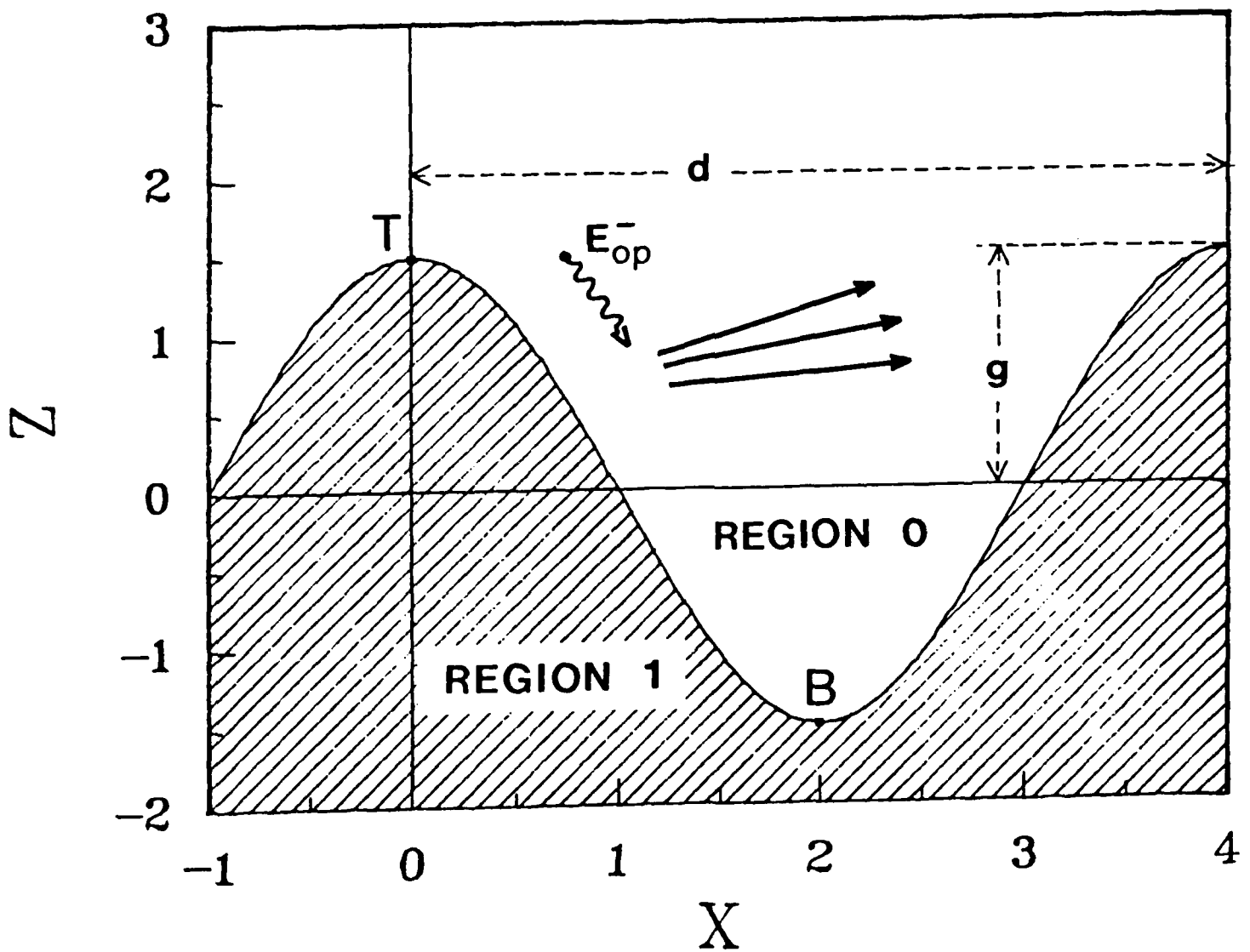
3
2
1
0
−1
−2
Z
−1
0
1
2
3
4
X
d
T
E_{op}^{-}
g
REGION 0
REGION 1
B

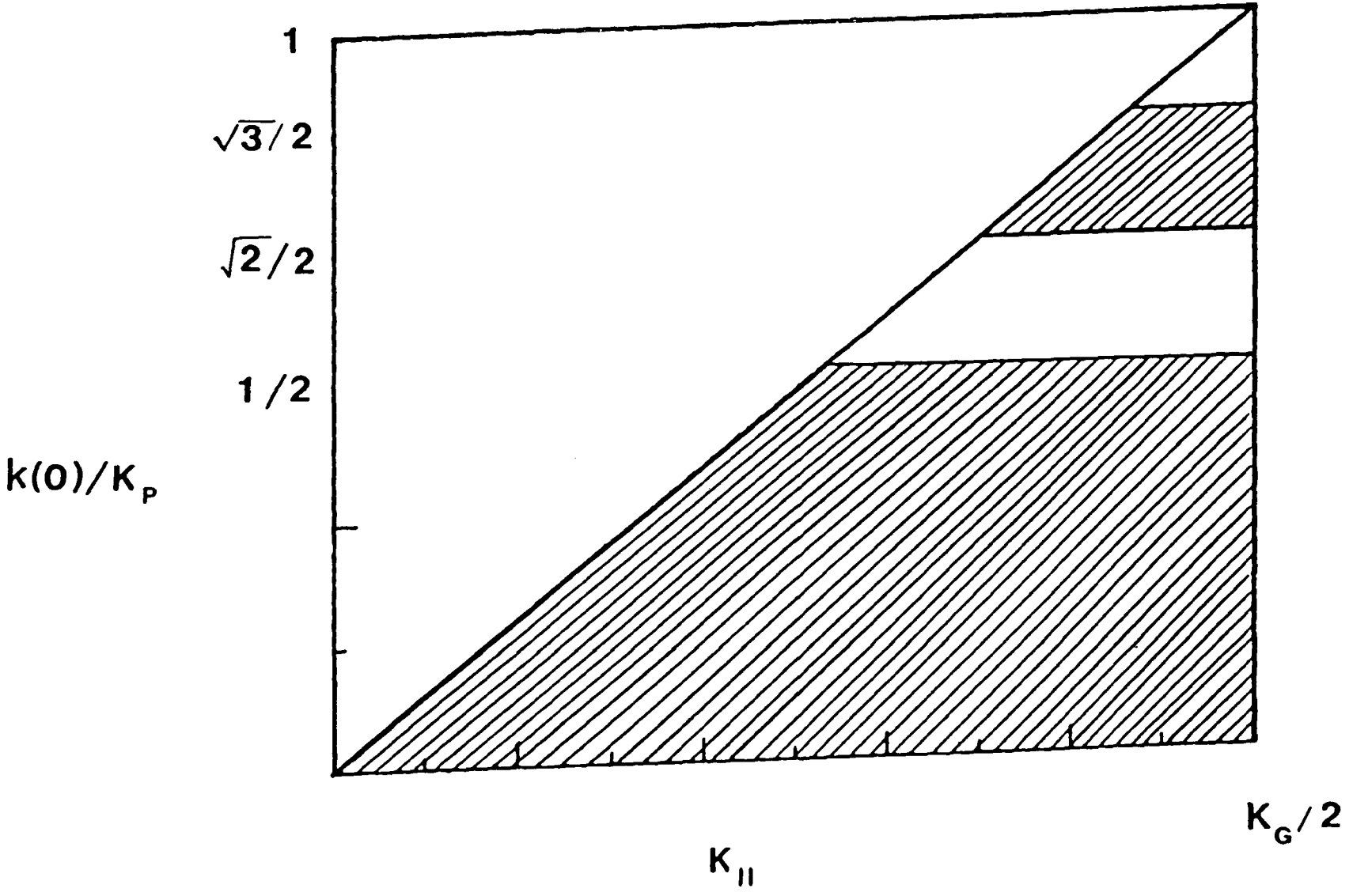

Fig 2

OL/413/83/01
GEN/413-2

TECHNICAL REPORT DISTRIBUTION LIST, GEN

	No. Copies
Office of Naval Research Attn: Code 413 800 N. Quincy Street Arlington, Virginia 22217	2
Dr. Bernard Douda Naval Weapons Support Center Code 5042 Crane, Indiana 47522	1
Commander, Naval Air Systems Command Attn: Code 310C (H. Rosenwasser) Washington, D.C. 20360	1
Naval Civil Engineering Laboratory Attn: Dr. R. W. Drisko Port Hueneme, California 93401	1
Defense Technical Information Center Building 5, Cameron Station Alexandria, Virginia 22314	12
DTNSRDC Attn: Dr. G. Bosmajian Applied Chemistry Division Annapolis, Maryland 21401	1
Dr. William Tolles Superintendent Chemistry Division, Code 6100 Naval Research Laboratory Washington, D.C. 20375	1
Dr. David Young Code 334 NORDA NSTL, Mississippi 39529	1
Naval Weapons Center Attn: Dr. Ron Atkins Chemistry Division China Lake, California 93555	1
Scientific Advisor Commandant of the Marine Corps Code RD-1 Washington, D.C. 20380	1
U.S. Army Research Office Attn: CRD-AA-IP P.O. Box 12211 Research Triangle Park, NC 27709	1
Mr. John Boyle Materials Branch Naval Ship Engineering Center Philadelphia, Pennsylvania 19112	1
Naval Ocean Systems Center Attn: Dr. S. Yamamoto Marine Sciences Division San Diego, California 91232	1
Dr. David L. Nelson Chemistry Division Office of Naval Research 800 North Quincy Street Arlington, Virginia 22217	1

DL/413/83/01
056/413-2

ABSTRACTS DISTRIBUTION LIST, 056/625/629

Dr. G. A. Somorjai
Department of Chemistry
University of California
Berkeley, California 94720

Dr. J. Murday
Naval Research Laboratory
Surface Chemistry Division (6170)
455 Overlook Avenue, S.W.
Washington, D.C. 20375

Dr. J. B. Hudson
Materials Division
Rensselaer Polytechnic Institute
Troy, New York 12181

Dr. Theodore E. Madey
Surface Chemistry Section
Department of Commerce
National Bureau of Standards
Washington, D.C. 20234

Dr. J. E. Demuth
IBM Corporation
Thomas J. Watson Research Center
P.O. Box 218
Yorktown Heights, New York 10598

Dr. M. G. Lagally
Department of Metallurgical
and Mining Engineering
University of Wisconsin
Madison, Wisconsin 53706

Dr. R. P. Van Duyne
Chemistry Department
Northwestern University
Evanston, Illinois 60637

Dr. J. M. White
Department of Chemistry
University of Texas
Austin, Texas 78712

Dr. D. E. Harrison
Department of Physics
Naval Postgraduate School
Monterey, California 93940

Dr. W. Kohn
Department of Physics
University of California, San Diego
La Jolla, California 92037

Dr. R. L. Park
Director, Center of Materials
Research
University of Maryland
College Park, Maryland 20742

Dr. W. T. Peria
Electrical Engineering Department
University of Minnesota
Minneapolis, Minnesota 55455

Dr. Keith H. Johnson
Department of Metallurgy and
Materials Science
Massachusetts Institute of Technology
Cambridge, Massachusetts 02139

Dr. S. Sibener
Department of Chemistry
James Franck Institute
5640 Ellis Avenue
Chicago, Illinois 60637

Dr. Arnold Green
Quantum Surface Dynamics Branch
Code 3817
Naval Weapons Center
China Lake, California 93555

Dr. A. Wold
Department of Chemistry
Brown University
Providence, Rhode Island 02912

Dr. S. L. Bernasek
Department of Chemistry
Princeton University
Princeton, New Jersey 08544

Dr. P. Lund
Department of Chemistry
Howard University
Washington, D.C. 20059

ABSTRACTS DISTRIBUTION LIST, 056/625/629

Dr. F. Carter
Code 6132
Naval Research Laboratory
Washington, D.C. 20375

Dr. Richard Colton
Code 6112
Naval Research Laboratory
Washington, D.C. 20375

Dr. Dan Pierce
National Bureau of Standards
Optical Physics Division
Washington, D.C. 20234

Dr. R. Stanley Williams
Department of Chemistry
University of California
Los Angeles, California 90024

Dr. R. P. Messmer
Materials Characterization Lab.
General Electric Company
Schenectady, New York 22217

Dr. Robert Gomer
Department of Chemistry
James Franck Institute
5640 Ellis Avenue
Chicago, Illinois 60637

Dr. Ronald Lee
R301
Naval Surface Weapons Center
White Oak
Silver Spring, Maryland 20910

Dr. Paul Schoen
Code 5570
Naval Research Laboratory
Washington, D.C. 20375

Dr. John T. Yates
Department of Chemistry
University of Pittsburgh
Pittsburgh, Pennsylvania 15260

Dr. Richard Greene
Code 5230
Naval Research Laboratory
Washington, D.C. 20375

Dr. L. Kesmodel
Department of Physics
Indiana University
Bloomington, Indiana 47403

Dr. K. C. Janda
California Institute of Technology
Division of Chemistry and Chemical
Engineering
Pasadena, California 91125

Dr. E. A. Irene
Department of Chemistry
University of North Carolina
Chapel Hill, Northc Carolina 27514

Dr. Adam Heller
Bell Laboratories
Murray Hill, New Jersey 07974

Dr. Martin Fleischmann
Department of Chemistry
Southampton University
Southampton SO9 5NH
Hampshire, England

Dr. John W. Wilkins
Cornell University
Laboratory of Atomic and
Solid State Physics
Ithaca, New York 14853

Dr. Richard Smardzewski
Code 6130
Naval Research Laboratory
Washington, D.C. 20375

Dr. H. Tachikawa
Chemistry Department
Jackson State University
Jackson, Mississippi 39217

DL/413/83/01
056/413-2

ABSTRACTS DISTRIBUTION LIST, 056/625/629

Dr. R. G. Wallis
Department of Physics
University of California
Irvine, California 92664

Dr. D. Ramaker
Chemistry Department
George Washington University
Washington, D.C. 20052

Dr. J. C. Hemminger
Chemistry Department
University of California
Irvine, California 92717

Dr. T. F. George
Chemistry Department
University of Rochester
Rochester, New York 14627

Dr. G. Rubloff
IBM
Thomas J. Watson Research Center
P.O. Box 218
Yorktown Heights, New York 10598

Dr. Horia Metiu
Chemistry Department
University of California
Santa Barbara, California 93106

Dr. W. Goddard
Division of Chemistry
California Institute of Technology
Pasadena, California 91125

Dr. J. T. Keiser
Department of Chemistry
University of Richmond
Richmond, Virginia 23173

Dr. R. W. Plummer
Department of Physics
University of Pennsylvania
Philadelphia, Pennsylvania 19104

Dr. E. Yeager
Department of Chemistry
Case Western Reserve University
Cleveland, Ohio 41106

Dr. N. Winograd
Department of Chemistry
Pennsylvania State University
University Park, Pennsylvania 16802

Dr. Roald Hoffmann
Department of Chemistry
Cornell University
Ithaca, New York 14853

Dr. A. Steckl
Department of Electrical and
Systems Engineering
Rensselaer Polytechnic Institute
Troy, NewYork 12181

Dr. G. H. Morrison
Department of Chemistry
Cornell University
Ithaca, New York 14853

Dr. P. Hansma
Physics Department
University of California
Santa Barbara, California 93106

Dr. J. Baldeschwieler
California Institute of Technology
Division of Chemistry
Pasadena, California 91125

ABSTRACTS DISTRIBUTION LIST, 056/625/629

Dr. J. E. Jensen
Hughes Research Laboratory
3011 Malibu Canyon Road
Malibu, California 90265

Dr. J. H. Weaver
Department of Chemical Engineering
and Materials Science
University of Minnesota
Minneapolis, Minnesota 55455

Dr. W. Goddard
Division of Chemistry
California Institute of Technology
Pasadena, California 91125

Dr. A. Reisman
Microelectronics Center of North Carolina
Research Triangle Park, North Carolina
27709

Dr. M. Grunze
Laboratory for Surface Science and
Technology
University of Maine
Orono, Maine 04469

Dr. J. Butler
Naval Research Laboratory
Code 6115
Washington D.C. 20375

Dr. L. Interante
Chemistry Department
Rensselaer Polytechnic Institute
Troy, New York 12181

Dr. Irvin Heard
Chemistry and Physics Department
Lincoln University
Lincoln University, Pennsylvania 19352

Dr. K.J. Klaubunde
Department of Chemistry
Kansas State University
Manhattan, Kansas 66506

Dr. W. Knauer
Hughes Research Laboratory
3011 Malibu Canyon Road
Malibu, California 90265

Dr. C. B. Harris
Department of Chemistry
University of California
Berkeley, California 94720

Dr. F. Kutzler
Department of Chemistry
Box 5055
Tennessee Technological University
Cookesville, Tennessee 38501

Dr. D. DiLella
Chemistry Department
George Washington University
Washington D.C. 20052

Dr. R. Reeves
Chemistry Department
Renssaeler Polytechnic Institute
Troy, New York 12181

END

FILMED

L-86

DTIC